AD NUMBER

AD825489

LIMITATION CHANGES

TO:

Approved for public release; distribution is unlimited.

FROM:

Distribution authorized to U.S. Gov't. agencies and their contractors; Critical Technology; DEC 1967. Other requests shall be referred to Air Force Office of Scientific Research, SRGO, Arlington, Va 22209. This document contains export-controlled technical data.

AUTHORITY

afosr ltr, 12 nov 1971

Service through Science

AFOSR No. 68-0002

FINAL TECHNICAL SUMMARY REPORT

December 1, 1965 -- November 30, 1967

AD825489

RESEARCH ON THE DEFLAGRATION OF HIGH-ENERGY SOLID OXIDIZERS

Contract No. AF 49(638)-1645

To:

Air Force Office of Scientific Research
Arlington, Virginia

2. This document is subject to special export controls and each transmittal to foreign governments or foreign nationals may be made only with prior approval of AFOSR (SRGL).

Kinetics and Combustion Group
Research Division

December 15, 1967

ATLANTIC RESEARCH

AFOSR No. 68-0002

Final Technical Summary Report

December 1, 1965 -- November 30, 1967

RESEARCH ON THE DEFLAGRATION OF HIGH-ENERGY SOLID OXIDIZERS

Contract No. AF 49(638)-1645

To:

Air Force Office of Scientific Research
Arlington, Virginia

Contributors: G. von Elbe, Chief Investigator
E. T. McHale

Consultants: R. Friedman
J. B. Levy

Kinetics and Combustion Group
Atlantic Research Corporation
A Division of The Susquehanna Corporation
Alexandria, Virginia

December 15, 1967

TABLE OF CONTENTS

I. INTRODUCTION AND SUMMARY

This report covers research performed during the past two years on the subject contract. It is a continuation of the study of solid oxidizer self-deflagration carried out under Contract No. AF 49(638)-1169 of the same title. In that program the deflagration behavior of hydrazine perchlorate (HP) and hydrazine diperchlorate (HDP) was investigated and is reported in references 1, 3, 4. The deflagration of hydroxylammonium perchlorate (HAP) was studied under the present program, the general objective of which was to gain some understanding of the deflagration process. The experimental work included measurements of the pressure dependence of the deflagration rate, flame temperature, quenching diameters, and inflammability limits. In this final report, included along with these results is a summary of the significant results of all the solid oxidizers which we have studied including also ammonium perchlorate (AP) and hydrazine nitroform (HNF). An analysis of the combustion process of these monopropellant-type oxidizers is presented, based on what has been determined, or can reasonably be inferred, about the structure of the combustion wave. The physical and chemical-kinetic processes beneath, at and in the gas above the surface of the solid are considered, the concept of cellular flame structure is discussed, and inflammability limits are analyzed.

The scope of the program also included a study of the extinguishment of propellants by rapid depressurization. In this phase of the work we developed a laboratory-scale extinguishment apparatus which was essentially a modified optical strand burner. This apparatus allows depressurization rates of up to 5×10^5 psi/sec at 2000 psi pressure. It has the advantages that data are obtained in a form suitable for testing extinction theories and also it can be used to study propellant extinguishment on strand-size samples. Three candidate composite propellants were selected for study and the results are compared with extinguishment theory, where the agreement is found to be good.

A study aimed at gaining some background knowledge in the general area of chlorine-oxide chemistry was also undertaken since this seemed relevant

to an underatanding of the perchlorate-based oxidizers. In this phaae of the work a review of the chlorine oxides and perchloric acid literature was carried out, and an experimental study of the explosive decomposition of chlorine dioxide waa performed. The resulta of the ClO_2 study together with an extensive interpretation of the reaction are presented in an appendix to this report. The studiea of all three phases of the program will be aubmitted for publication.

II. THE DEFLAGRATION OF SOLID OXIDIZERS

A. SUMMARY OF PERTINENT RESULTS ON FIVE OXIDIZERS

Some physical and chemical properties of the crystalline materials are listed in Table I. Below are presented the experimental results of our deflagration studies which are relevant for an analysis of the combustion process. We omit a formal description of the experimental details since for the most part they were standard methods and have been previously described; where appropriate, mention is made of the general techniques employed.

1. Deflagration Rates

In Figure 1 are presented in a log-log diagram the mass burning rates versus pressure for the five monopropellants. The n's refer to the exponent in the equation

$$\dot{m} = bp^n \qquad (1)$$

where $\dot{m}$ is the mass burning rate in $g/cm^2 sec$ and p is pressure in atm. The data from which Figure 1 is constructed are given in references 2-5 for AP, HP, HDP and HNF, respectively. The actual data for HAP have not been published and they are presented in Figure 2. In this figure the dashed lines are only meant to indicate the irreproducibility of data below 200 atm. The measurements for all the oxidizers were made on strands compacted to high density and burned at room temperature in an optical strand burner. In Figure 1 the line for HP refers to the material containing small amounts of additives since reproducible data were never obtained for pure HP. The following descriptive comments are made about the deflagration of the oxidizers. HP, HDP and HNF all melt as they enter the deflagration wave at the lower pressures, but the liquid layer is not observable at the higher pressures. HAP melts readily but no liquid layer was observable during burning since deflagration below about 150 atm does not occur unless the material is preheated. In the case of AP, HAP and HF the lowest point of the line represents the lower pressure limit for deflagration; HNF and HP burned at as low

TABLE I

PROPERTIES OF SOLID OXIDIZERS

Compound	Formula	Crystal Density (g/cc)	Color	Molecular Weight	Melting Range (°C)	ΔH_{vap} kcal/mole	ΔH_{vap} cal/g	Temp. at which** v.p. is 1 atm (°C)
Ammonium perchlorate (AP)	NH_4ClO_4	1.95	White	117.5	--	58	493	545
Hydroxylammonium perchlorate (HAP)	$HONH_4ClO_4$	2.06	White	133.5	85-90	33*	247	375
Hydrazine perchlorate (HP)	$N_2H_5ClO_4$	1.94	White	132.5	140-142	58	438	625
Hydrazine diperchlorate (HDP)	$N_2H_6(ClO_4)_2$	2.21	White	233	190-192	95***	407	--
Hydrazine nitroform (HNF)	$N_2H_5C(NO_2)_3$	1.87	Orange	183	120-132 with decomposition	--	--	--

* Assumes no dissociation; data from reference 6.

** Calculated from references 3 and 7.

*** By extrapolation of vapor pressure-temperature data.

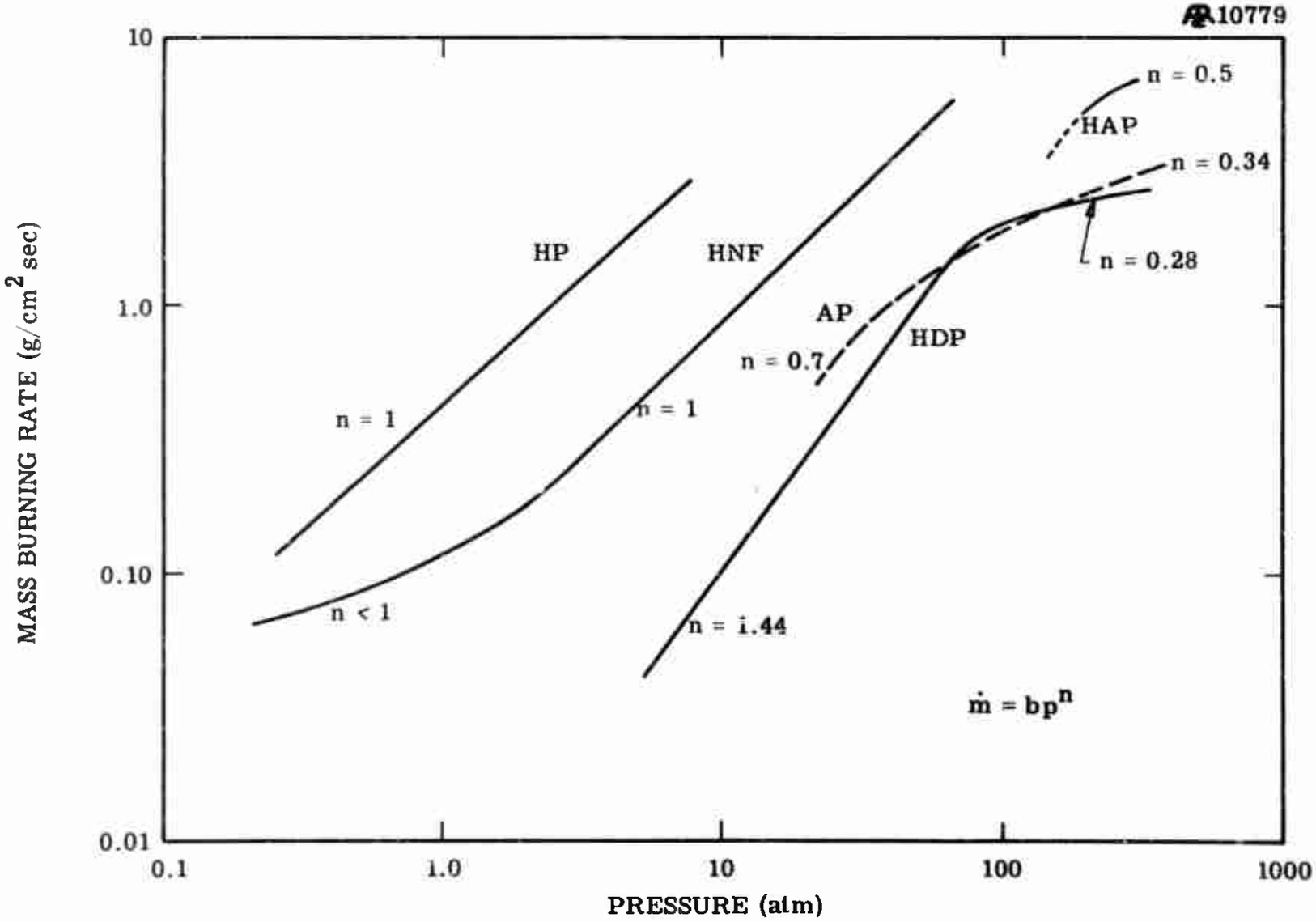

Figure 1. Log-Log Plot of Self-Deflagration Rate Versus Pressure for Five Solid Oxidizers.

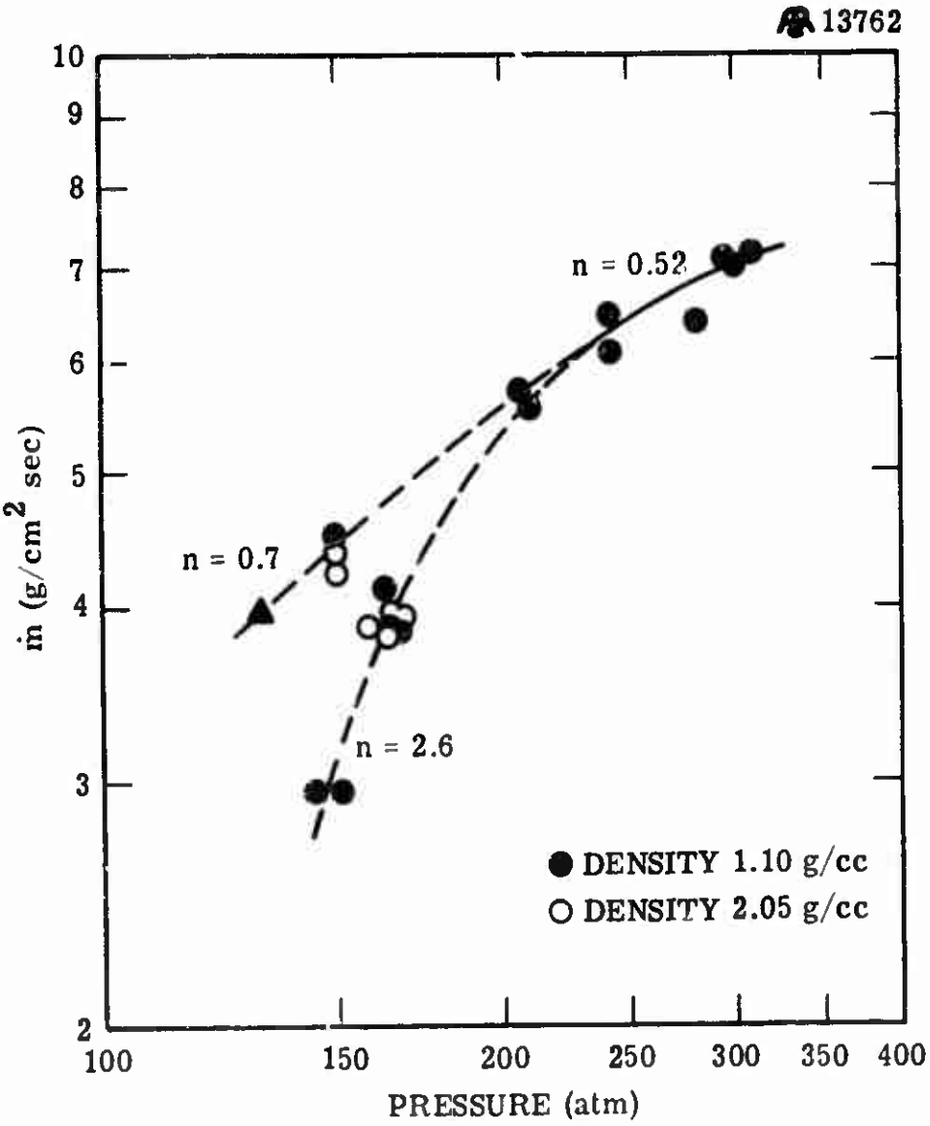

Figure 2. Mass Deflagration Rate Versus Pressure for Hydroxylammonium Perchlorate.

as tenths of an atmosphere and no lower limit was determined. No upper limits were observed except for HP, where deflagration above approximately 8 atm could never be effected. Other features of Figure 1 are discussed in the following section.

2. Flame Temperatures and Reaction Stoichiometries

The adiabatic, constant pressure product gas temperatures and equilibrium compositions have been calculated for the five oxidizers and are summarized in Table II. The initial temperature was 25°C and the heats of formation and reaction are listed. The approximate computed compositions are shown as reaction equations and species present only in minor concentrations are omitted. The experimentally determined flame temperatures are also presented. These were measured with fine thermocouples except for the case of HP where the sodium line-reversal technique was used. We can now remark on certain features of the relative burning rates of Figure 1.

The only oxidizer that exhibits an exponent greater than unity is HDP at pressures below about 80 atm. This has previously been explained (4) qualitatively as due to the flame standoff distance becoming shorter with increasing pressure coupled with an increase in flame temperature. The exponent decreases to <1 as the flame temperature levels off at the theoretical value. HP exhibits much faster burning rates than HNF even though the calculated flame temperature and heat of reaction of HNF are higher. This illustrates the role of the reaction kinetics in determining the relative deflagration rates of these two oxidizers, which is analyzed below.

Examining the plots of Figure 1 in the light of only the thermodynamics data of Tables I and II, one finds one other fairly gross departure from first expectation. We note that HAP, when it burns, burns several times as fast as AP. Since HAP has a higher T_f and lower ΔH_{vap} and probably a lower surface temperature, faster deflagration rates are reasonable. However, HAP has a low-pressure limit which is at least seven times higher than AP. To account for this feature we have postulated that condensed-phase heat release is necessary to drive the combustion. The pressure dependence of the

TABLE II

Thermodynamic Combustion Data for Solid Oxidizers

Oxidizer	T_f (°K) Computed	T_f (°K) Measured	ΔH_f (Kcal/mole)	ΔH_{rx} (Kcal/mole)	ΔH_{rx} (Cal/g)
AP	1440 (100 atm)	1205 (100 atm)	- 69.4	- 40.6 (theo) - 34 (actual)	-350 (theo.) -290 (actual)
HAP	1413 (200 atm)	1305 (200 atm)	- 66.5	- 44.0	- 330
HP	2245 (1 atm)	2275 (1 atm)	- 42.5	- 95	- 720
HDP	1600 (28 atm) 1600 (55 atm) 1605 (103 atm)	1345 (28 atm) 1520 (55 atm) 1595 (103 atm)	- 70.1	- 88	- 380
AlF	2765 (1 atm)	--	- 17.0	- 178	- 970

Flame Reactions

$NH_4ClO_{4(s)} \rightarrow 0.5N_2 + 1.6\ H_2C + 0.8\ HCl + 0.1\ Cl_2 + 1.2\ O_2$ (100 atm theoretical)

$\rightarrow 0.27\ N_2 + 1.6\ H_2O + 0.8\ HCl + 0.1\ Cl_2 + 0.12\ N_2O + 0.23\ NO + 1.0\ O_2$ (measured at 70 atm)

$HONH_4ClO_{4(s)} \rightarrow 0.5\ N_2 + 1.6\ H_2O + 0.8\ HCl + 0.1\ Cl_2 + 1.7\ O_2$ (200 atm)

$N_2H_5ClO_{4(s)} \rightarrow 0.98\ N_2 + 2.0\ H_2O + 0.93\ HCl + 0.01\ Cl_2 + 0.05\ Cl + 0.03\ OH + 0.04\ NO + 0.95\ O_2$ (1 atm)

$\doteq N_2 + 2\ H_2O + HCl + O_2$

$N_2H_6(ClO_4)_{2(s)} \rightarrow 1.0\ N_2 + 2.0\ H_2O + 2.0\ HCl + 3.0\ O_2$ (100 atm)

$N_2H_5\ C(NO_2)_{3(s)} \rightarrow 2.44\ N_2 + 2.17\ H_2O + 0.72\ CO_2 + 0.28\ CO + 0.35\ OH + 0.12\ NO + 0.77\ O_2$ (1 atm)

deflagration rates arises because heat is also released in the gas phase and feedback from the gas reaction zone is in turn necessary to drive the condensed-phase reactions. This is a reasonable qualitative explanation for the phenomena but the relative degrees of condensed-phase and gas-phase heat release could not be determined.

3. Temperature Profiles

The technique of imbedding fine thermocouples in compacted oxidizer strands and allowing the deflagration wave to overrun the bead was used to determine temperature profiles. One criterion that must be fulfilled to obtain valid profiles with adequate spatial resolution is that the thermocouple bead size must be small compared with the characteristic combustion wave thickness, α/r, where α is the thermal diffusivity of the solid and r is the linear burning rate. This limits profile determinations to deflagrations of a few tenths of a cm/sec and less for reasonable-sized couples. Hence, profiles were not measured for AP and HAP, but were for HP, HDP and HNF at low pressures. Even for these three it was not possible to resolve temperature near the surface since gradients in this region are very high.

At relatively low pressures and slow burning rates the temperature profiles through the preheat zones of HNF and HDP showed definite evidence for substantial heat release well below the surface. For these two materials, chemical reactions in the liquid layer are the principal driving force of the deflagrations at low pressures. In the case of HP there seemed to be minimal heat release at any great depth beneath the strand surface. The profiles for these oxidizers have previously been published and discussed (3,4,5) and for purposes in this report we only wish to consider one additional property of the profiles. That is the total width of the preheat zone compared to the characteristic dimension of the combustion wave, α/r. In all cases the preheat zone was found to be approximately 5-7 times α/r. This is substantially the order of magnitude of the analogous ratio in gaseous flames and is an important consideration in inflammability limits.

4. Quenching Diameters

Under the present program we have measured quenching diameters for AP and HAP deflagrations as a function of pressure, and similar data were obtained for HNF under a different but similar program (5). The experiments

consisted of compacting the crystalline oxidizers into Pyrex tubes of a range of diameters, then determining the lowest pressure at which deflagration would propagate for a given diameter. The data for HNF are given in reference 5 and the quenching curve is shown on the summary graph of Figure 7 which will be discussed in the next section. The results for AP were anomalous and do not lend themselves to straightforward analysis in some respects. Accordingly we present the actual data for AP in Figures 3 and 4, and for comparison with an example of "clean" data the results for HAP are given in Figure 5. The burning rates vary with sample diameter (and particle size for AP), and these were measured for the oxidizers. The AP rates are given in Figure 6 where only enough data were taken to satisfy the needs of this particular study; the HAP rates are given in Table III for deflagration at 200 atm. In the Table it is seen that a monotonic increase

TABLE III

Mass Burning Rates of HAP at 200 atm as a Function of Tube Diameter ($\rho \sim 1.1$ g/cm^3)

Pyrex Tube i.d. (mm)	$\dot{m}$ (g/cm^{2}sec)
3.8	4.08 4.24
5.8	4.52 4.63
8.0	5.25 (avergage of several)

in $\dot{m}$ with increasing tube diameter continues even up to 8 mm i.d. tubes, which exceed the quenching diameter by a factor of three at 200 atm. The pressure exponent of Figure 1 for HAP deflagration could be on the high side because of this, and the low value of the measured flame temperature may also be partially due to it.

The legends on Figures 3, 4, and 5 make the plots fairly self-explanatory. Lines are shown along which the Reynolds number is calculated to be 2300, indicating that the HAP flame gas stream is well in a turbulent

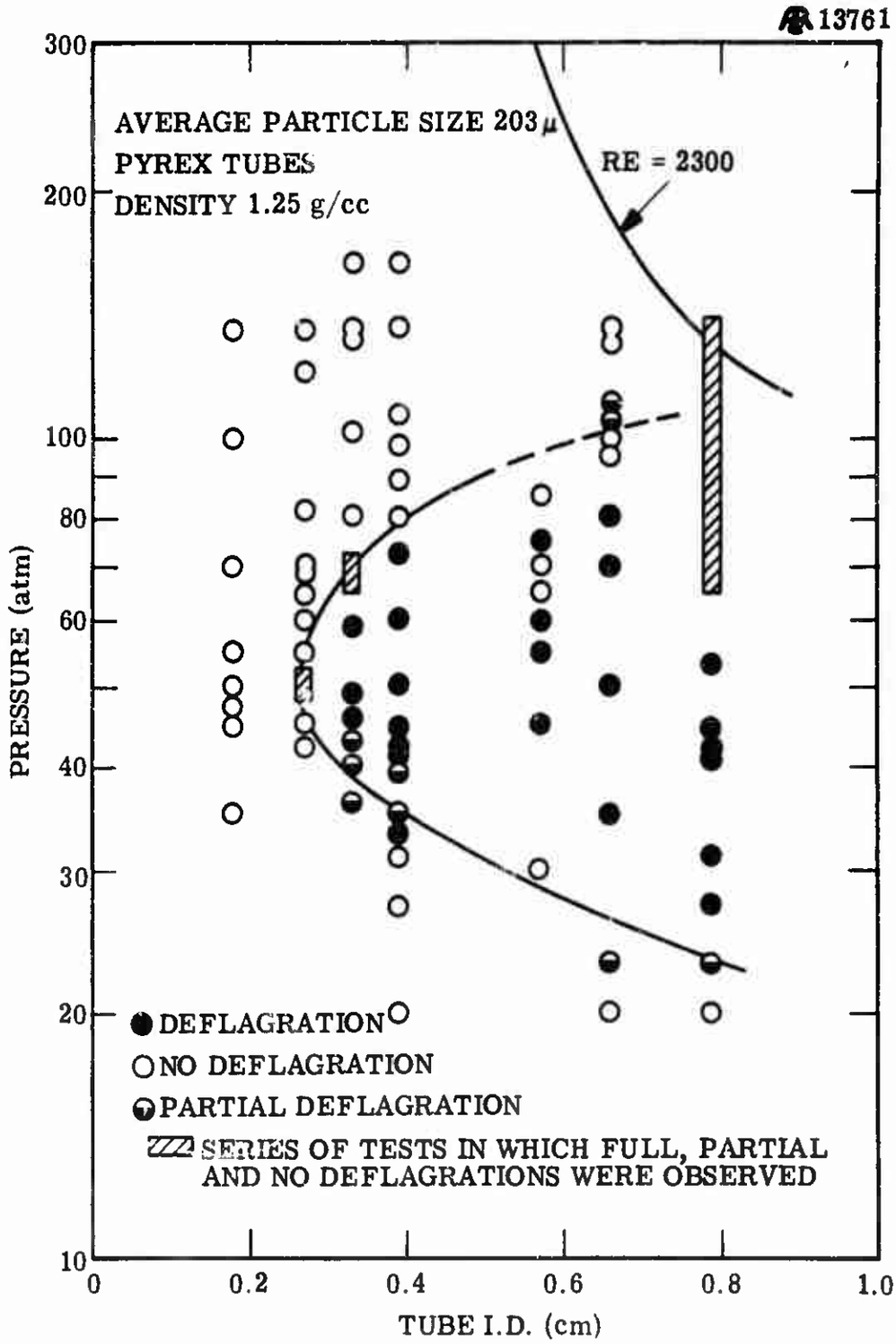

Figure 3. Quenching Diameters Versus Pressure for AP.

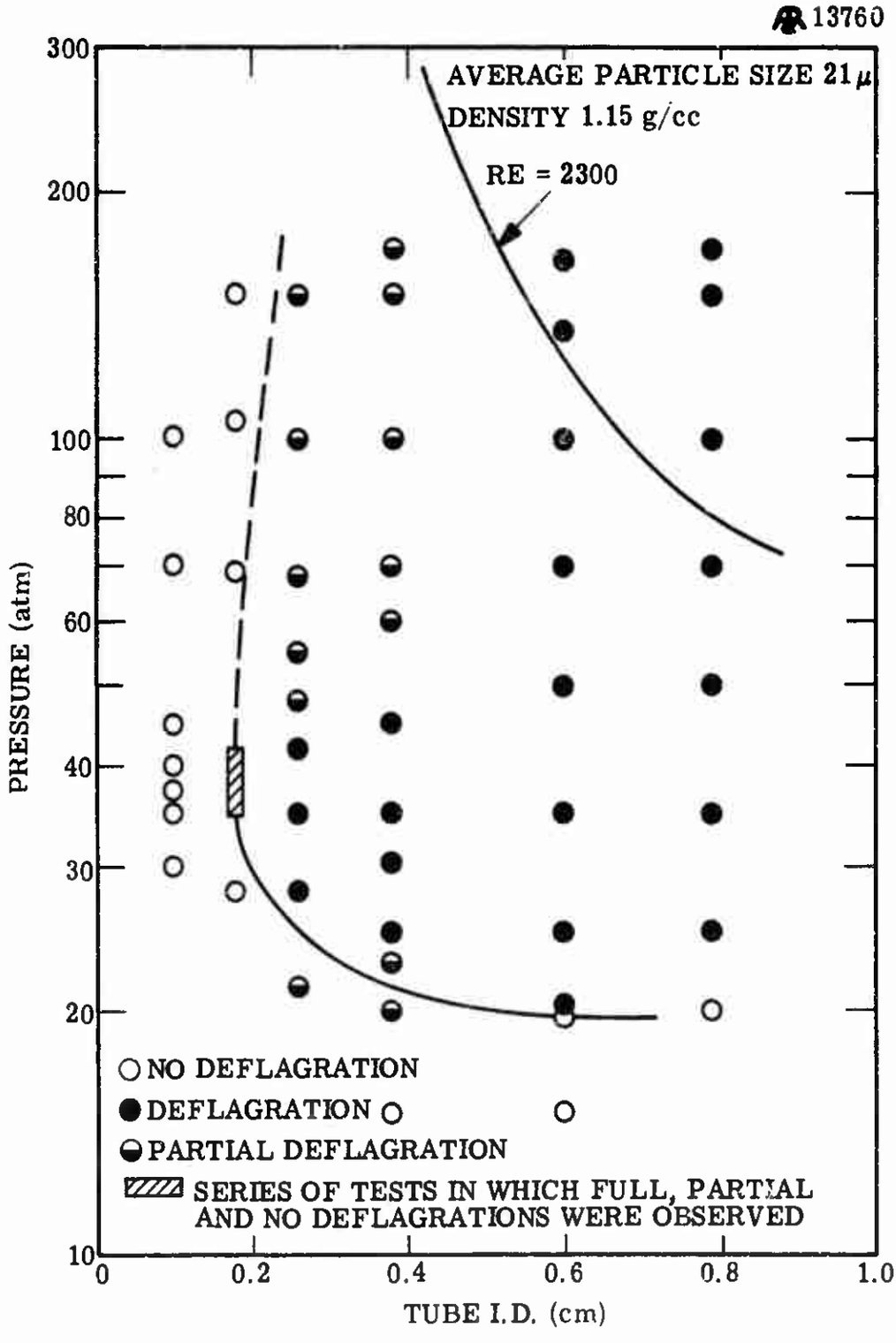

Figure 4. Quenching Diameters Versus Pressure for AP.

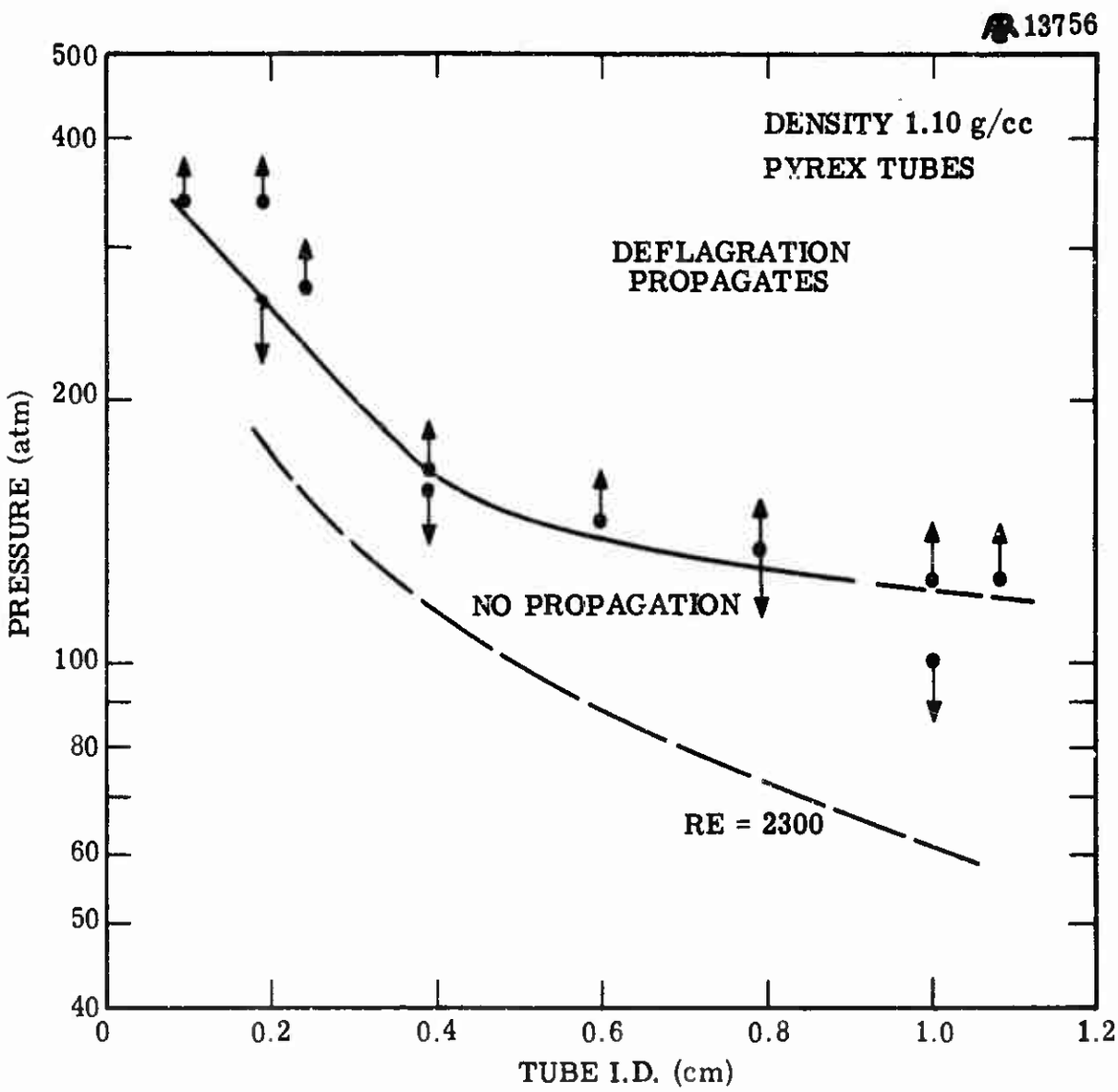

Figure 5. Quenching Diameters Versus Pressure for HAP.

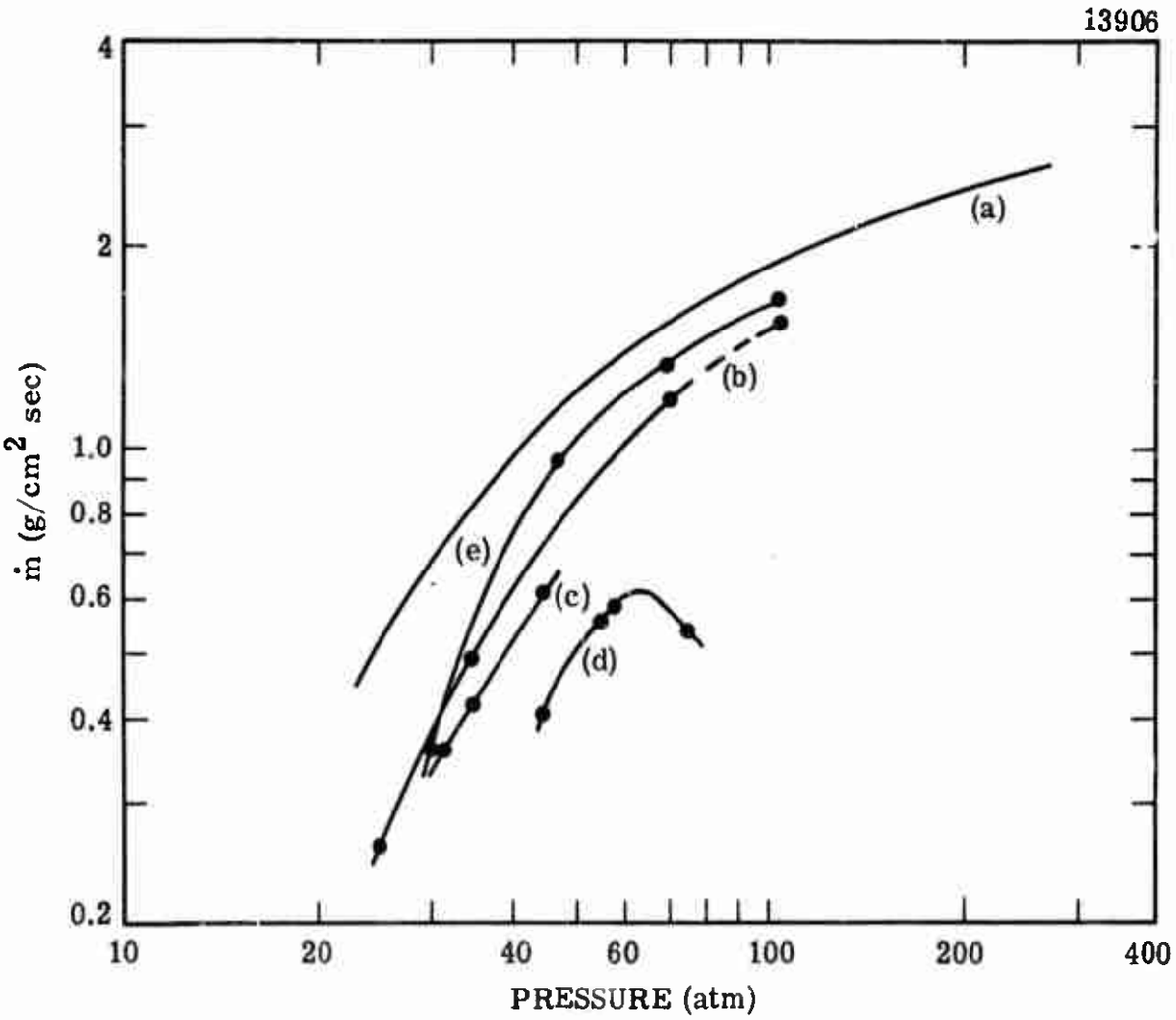

Figure 6. Mass Deflagration Rate Versus Pressure for AP. (a) Data from Reference 3 for Compacted Strands Near Crystal Density; (b) 21μ AP, 1.15 g/cc Density, 6mm Pyrex Tubes; (c) 21μ AP, 1.15 g/cc Density, 3.3mm Pyrex Tubes; (d) 203μ AP, 1.28 g/cc Density, 5.7mm Pyrex Tubes.

16940

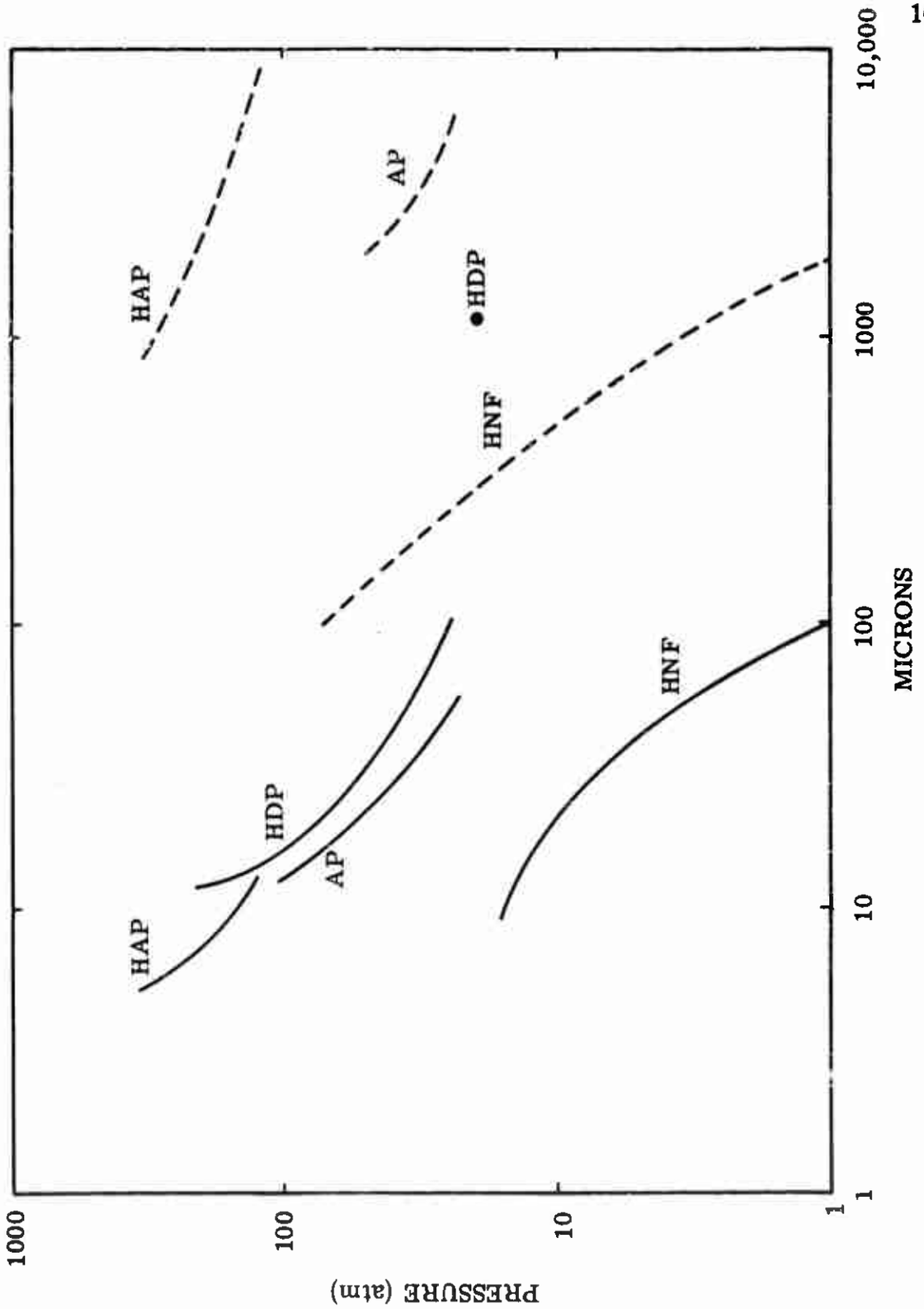

Figure 7. Characteristic Wave Width (solid lines) and Pyrex Tube Quenching Diameter (dashed lines).

region and that of AP in laminar. ideally one would expect to find the quenching diameter decreasing with increasing pressure as with HAP and HNF. For AP of 200μ particle size the line clearly turns back on itself in the region of 50 atm and 3 mm diameter tubes. In Figure 3, for 20μ AP, this is not quite the case although deflagration did not propagate at any pressure in tubes of less than 2 mm diameter. We have not had much success in understanding the curious feature of the AP curves, but the quenching results in general can be analyzed in terms of the dimensions of the deflagration wave in the same way that quenching distances are for gas flames.

B. DISCUSSION AND ANALYSIS OF THE COMBUSTION PROCESS

In this section we wish to discuss three aspects of the combustion process of solids: namely, quenching distances and inflammability limits; cellular flame structure; and the kinetics of the gas reaction and their relation to the deflagration rate. These subjects have not received appreciable attention heretofore, with the exception of the kinetics topic which has been analyzed by Friedman (8) for AP using an approach not too dissimilar from that taken here.

1. Quenching Diameters and Inflammability Limits

A summary of the quenching results is presented in Figure 7. The dashed lines are the experimental quenching diameters of AP, HNF and HAP; the solid lines are the calculated characteristic combustion wave dimensions, $\alpha/r = \lambda$, for the four oxidizers considered. The thermal diffusivities were estimated, based on the measured α's for AP (9). The • shown on the plot represents one experimental quenching diameter value for HDP deduced from reference 4. In the case of AP the quenching line is approximate based on Figures 3 and 4.

The quenching diameter for a combustion system depends on the thermal diffusivity and initial temperature of the quenching wall material. For gas flames, quenching diameters measured in glass or metal tubes are usually found to be of the order of 20-50 times and sometimes more the characteristic wave dimension α/Su. The explanation of the 20-50 factor is that the effective

combustion (half) wave width is some multiple of α/S_u (typically 5-10) and for a wave to propagate in a channel, the width of the channel must accommodate at least a full wave. When the lateral dimension (channel width) spprosches the combustion wave width, heat loss prevents propagation. As previously mentioned we have determined that the actual (half) wave width for the oxidizers in $\sim$5-7 times α/r. In Figure 7 it is seen that the quenching diameters are fairly constsnt multiples of α/r, which are $\sim$20 for HNF, $\sim$90 for AP and $\sim$200 or more for HAP. The dsta all refer to material compscted to roughly the same density into Pyrex tubes and should be comparable on the same basis. HNF exhibits quenching diameters in excellent agreement with what would be predicted from normal gas flames. AP quenching diameters are somewhat large compared to those of gaseous systems, and HAP are excessively larger. We feel that the large values for AP and HAP may be related to the cellular structure that these systems probably exhibit (see following section). In addition, HAP deflsgration very likely proceeds with substantial condensed-phase hest release even st high pressure and this may contribute in some way to the sbnormally high quenching diameters. However these observations currently stand as problems that require further resesrch.

A word can be added concerning the low-pressure inflammability limits of AP and HAP of 20 and 146 atm, respectively. There has always been a question as to whether these are absolute limits (at least in the case of AP) or limits set by sample dimensions and ignition. It was hoped that the quenching diameter study would cast light on this problem, however, the results do not really advance the knowledge in this area very greatly. Perhaps they favor the sbsolute-limit case since as the limits are approached the quenching diameter-pressure curves seem to flatten out, especially in the HAP system, but this is a weak argument at best.

We have made some calculations of the ignition requirements for AP and these are included because they illustrate that ignition could be a problem at lower pressures. As an example, consider what conditions must be met to effect self-sustaining deflagration of AP at, say, 10 stm, i.e., a 50% reduction of the limit. The ignition requirement can be estimated from the equation of thermsl

ignition theory (13);

$$\sqrt{\tau}\, f \doteq \sqrt{C_p \rho \lambda}\,(T_s - T_o) \qquad (2)$$

τ is the length of time that a heat flux f must be applied to a solid of heat capacity, density and thermal conductivity C_p, ρ and λ, respectively, to raise its surface temperature to T_s from T_o. τ is the ignition lag in the thermal theory and can be approximated by the characteristic combustion residence time, α/r^2. Then f is the proper flux to produce the steady-state preheat. The right side of the equation is practically independent of pressure, and for a T_s of 525°C and T_o of 25°C and using data from (9) for C_p, ρ and λ, it has a value of approximately 15 cal/cm^2 sec$^{1/2}$. τ at 10 atm would be $\sim$0.1 sec, hence f is computed to be $\sim$50 cal/cm^{2}sec. This is a readily attainable flux, but one would want to apply it to a sample of fairly large area, possibly a few square centimeters. This therefore puts restrictions on the ignition source. If a solid propellant were considered, for example, one can estimate from the previous equation that the flux would be of the order of 250 cal/cm^{2}sec for 0.004 sec, for a typical burning rate for propellants of 0.5 cm/sec at 10 atm. The calculations therefore show that an under-ignition condition could easily prevail if care were not taken to insure proper ignition of AP at low pressure.

2. Cellular Flame Structure

In the course of our studies of the self-deflagration of solid oxidizers and the analysis of the results in terms of the structure of combustion waves, we have been led to the conclusion that ammonium perchlorate must exhibit cellular structure. Cellular flames have long been known for gaseous combustion mixtures and are discussed in reference (14). They spontaneously form when the combustible mixture is stoichiometrically unbalanced and the diffusivity of the deficient component is higher than that of the component in excess. The ammonium perchlorate system meets these criteria, being oxidizer rich, and NH_3 having a much higher diffusivity than the $HClO_4$ component. Under these conditions cells would be expected to form, and the diffusional stratification of gasified reactants would yield a mixture of NH_3

and $HClO_4$ which is richer in NH_3 within the cell and more stoichiometrically balanced. The burning velocity will therefore be higher within than between cells where the reactant mixture will be very fuel lean. Correspondingly, the heat flux back to the solid will be greater within the cells. During the burning of a single crystal of AP, cellular flames would be expected to engrave a pattern on the surface. Such an engraved pattern has been found by Price and Hightower (15) in their studies of the deflagration of single AP crystals, in which they quenched the combustion and examined the surface.

Another criterion which we believe must be met for cellular flames to form is the lateral diffusion distance of an element of reactant should be comparable to or larger than the reaction zone thickness. For AP at 80 atm pressure a one-dimensional treatment such as given below yields a reaction zone of about one micron. An average lateral diffusion distance, x, can be estimated from

$$x = \sqrt{2Dt} = \sqrt{2Dy/v_g} \qquad (3)$$

where D is the diffusivity of NH_3 estimated to be 0.015 cm^2/sec at 1000° and 80 atm, t is the average time spent in the reaction zone estimated as y/v_g where y is ~1 micron and v_g is the average gas velocity which we calculate to be approximately 35 cm/sec. x therefore is ~3 microns, and the ratio x/y is about 3. For the cellular flames of butane-air studied by Markstein (16) we estimate the analogous x/y ratio to be about 2. This criterion seems therefore to be at least as well fulfilled for the AP system. We further can estimate the cell size to be of the order of 100 times the reaction zone thickness based on comparison with the butane-air cells. This would predict a cell size at 80 atm of ~50μ, which is approximately the dimension of the engraved pattern observed by Price and Hightower at 80 atm.

Cellular structure may be an important consideration when interpreting some combustion behavior of AP. It is likely not to be important when considering the burning of a single AP particle embedded in a propellant binder matrix. Also in the deflagration of pressed strands of the oxidizer made from AP of various particle sizes it may become washed out. Conditions are

fulfilled to a greater or lesser extent in the other monopropellant-type oxidizer systems for formation of cellular flames although they too may be washed out and never observed by the melting and heterogeneity of the samples. It does not seem profitable to analyze the other oxidizers as was done above for AP since no experimental evidence exists for cellular flames with these materials.

At this point we add the clarification that in spite of the cellular structure we believe AP and possibly the other systems exhibit, it is still valid for some conceptual purposes to discuss the combustion process in a one-dimensional model. In such instances a space-time averaging out of the microstructure of the wave represents a useful simplification.

3. Gas Reaction Zone Kinetics

The physical model for the self-deflagration of the oxidizers can be specified as follows: In the steady state the crystalline material gasifies as a result of heat conducted to it from a gas reaction zone. The vaporized reactants enter the flame, react exothermically, and heat flux back to the solid maintains the reactant supply. Thus the process is self-sustaining and the crystal ablates at a constant rate. Such a process should exhibit a positive pressure exponent, which is observed experimentally. The surface will maintain itself at an approximately constant temperature, although the magnitude of the surface temperature is unknown, as is its variation with pressure, if any, except in the case of AP where at least the general magnitude of the surface temperature is somewhat settled (17, 18). Gasification may occur by dissociative evaporation or by decomposition to some greater or lesser extent into intermediate species, the former mode being most often assumed and the latter being the mode which would give rise to condensed-phase heat release. The various modes of oxidizer gasification have been discussed (19).

The model can be formulated mathematically by writing a one-dimensional heat balance at the surface:

$$\lambda \left.\frac{dt}{dx}\right)_g = \dot{m} \left[C_p (T_s - T_u) + \Delta H_{vap} - Q_{c\phi}\right] \tag{4}$$

The left-hand term is the heat flux from the gas flame and this must equal the rate at which the convective sensible heat plus the heat of vaporization less

any condensed-phase heat liberation must be maintained. If we approximate the temperature gradient in the gas phase as linear, then

$$\dot{m} = \frac{\lambda (T_f - T_s)}{L [C_p(T_s - T_u) + \Delta H_{vap} - Q_{c\phi}]} \qquad (5)$$

The term we are most interested in is L, the gas reaction zone thickness. Ignoring for the moment $Q_{c\phi}$, we can calculate L from equation (5) for AP using the following measured values: T_f, 930°C[2]; T_s ~530°C[17]; $C_p(T_s - T_u)$, 150 cal/g; ΔH_{vap}, 500 cal/g[20]; λ, 0.0002 cal/cm sec deg (estimated). At 35 atm, for example, where $\dot{m}$ is 0.8 g/cm^{2}sec, L is found to be 2 microns. If condensed-phase heat release is included and arbitrarily assumed equal in magnitude to ΔH_{vap}, then L is computed to be 7 microns. One can also calculate from simple kinetic theory and an average gas velocity, temperature and molecular weight, that at 35 atm a reactant molecule makes on the average of the order of 10^5 collisions while passing through the flame zone.

It is of interest to estimate L for the other oxidizers and the results are given in Table IV. T_s was taken as 600°C for all cases and C_p and λ were taken as 0.3cal/g deg and 2×10^{-4} cal/cm sec deg. ΔH_{vap} is given in Table I except for HNF which was estimated to be 400 cal/g. The L's refer to $\dot{m}$ = 2 g/cm^{2}sec, and no condensed-phase heat release was assumed.

TABLE IV

Estimation of Gas Reaction Zone Thickness for Solid Oxidizers at $\dot{m}$ = 2 g/cm^{2}sec

Oxidizer	L (microns)
AP	0.5
HAP	1.0
HP	2.0
HDP	1.0
HNF	3.0

The magnitude of all the L's is seen to be of the order of one micron, although individual values differ by as much as a factor of six. We note that

a bad estimate of T_s would not substantially affect the results, although a very bad estimate of $Q_{c\phi}$ would have a significant effect.

Next we turn to a consideration of what overall reaction kinetics are required to produce flame zones of this order of magnitude in size. Let us assume that reactants leave the surface of the solid at T_s, pass through a non-isothermal reaction zone of thickness L cm at an average velocity $\bar{v}$ cm/sec, and emerge as combustion products at T_f. We consider two cases: a reaction first-order overall in one of the species, and a reaction first-order in each of two species with equal initial concentrations (which is equivalent to a second-order reaction in one species). Then,

$$-\frac{d[a]}{dt} = k_1[a] \text{ or } k_2[a]^2 \tag{6}$$

Neglecting the minor effect of density change with temperature and also diffusional effects, and introducing the Arrhenius expressiou for k, (6) becomes for first order,

$$\ln\left([a_o]/[a]\right) = -\ln(1-F) = \int_o^t A \exp[-E/RT(t)]\, dt, \tag{7}$$

and for second order,

$$\frac{F}{[a_o](1-F)} = \int_o^t A \exp[-E/RT(t)]\, dt \tag{8}$$

where F is the fraction of a reacted and T is a function of distance through the non-isothermal zone.

The approximation that T increases linearly allows us to write

$$T = T_s\,[\,1 + \beta \bar{v}\, t\,] \tag{9}$$

where $\bar{v} = \dot{m}/\bar{\rho}_g$ and $\beta = (T_f - T_s)/T_s L$, so that the right side of (8) can be written

$$\int_0^{t_L} A \exp\left[-E/RT_s\ (1 + \beta\ \bar{v}\ t)\right]\ dt \qquad (10)$$

In order to integrate, the term $(1 + \beta\ \bar{v}\ t)^{-1}$ can be approximated as $(1 - \beta\bar{v}t/m)$ where m is a constant adjusted for each oxidizer (see Table V for values). Then (10) becomes

$$k_s \int_0^{t_L} \exp\left[E\ \beta\ \bar{v}\ t/m\ RT_s\right] dt \qquad (11)$$

which integrates to

$$A \exp\left[-E/RT_s\right]\left[m\ RT_s/E\ \beta\ \bar{v}\right]\left|\exp\left[E\ \beta\ \bar{v}\ t_L/m\ RT_s\right] - 1\right| \qquad (12)$$

The minus one term is negligible (so long as the value of the exponent is greater than about unity), hence,

$$-\ln\ (1 - F) \text{ or } \frac{F}{[a_o](1-F)} = A\left[\frac{mRT_s}{E\beta\bar{v}}\right] \exp\left\{-\frac{E}{RT_s}\left[1 - \frac{\beta\bar{v}t_L}{m}\right]\right\} \qquad (13)$$

Using equation (13) one may calculate "global" activation energies for the gas reactions of the oxidizers. We have done this and the pertinent input data and results are shown in Table V. We have taken the pre-exponential factors as 10^{13} sec^{-1} and 10^{14} cc/mole sec for first- and second-order reactions respectively, and required F to be 0.99. The calculations are for $\dot{m}$ = 2 $g/cm^2 sec$ for all the oxidizers and the previous values of L were used which refer to an assumed T_s of 875°K and $Q_{c\phi}$ = 0. At this point, to avoid any confusion, we emphasize that in reality HNF and HDP exhibit substantial $Q_{c\phi}$ at low pressure and this is necessary to drive the deflagration. At high pressure, the extent of $Q_{c\phi}$ for HNF and HDP is unknown, but we believe HAP exhibits $Q_{c\phi}$ at high pressure and failure to sustain condensed-phase reactions

TABLE V

Data and Results for Analysis of Kinetics of Oxidizer Flame Zones

Ox.	$\beta \times 10^{-3}$ (cm^{-1})	$\bar{v}$ (cm/sec)	$t_L \times 10^6$ (sec)	m	E (Kcal/mole)	
					1st Order	2nd Order
AP	7.55	38	1.32	1.5	32	16
HAP	4.93	36	2.78	1.5	36	19
HP	7.83	1160	0.172	2.5	46	7
HDP	8.28	34	2.94	1.5	50	24
HNF	10.8	214	1.40	4.5	73	24

may be the cause of the high low-pressure limit. However in the treatment presented in this section, setting $Q_{c\phi} = 0$ is a justified approximation since the errors it introduces are tolerable for our purposes. They would not be if a very accurate treatment were attempted.

To get some idea of the approximate overall order of each reaction, the L in equation (5) can be approximated by the energy balance:

$$L = \frac{\dot{m} [C_p (T_f - T_u) + \Delta H_{vap} - Q_{c\phi}]}{\dot{Q}} \qquad (14)$$

where $\dot{Q}$ is an average reaction rate through the gas zone. From (14) and (13) it is found that

$$\dot{m}^2 \propto \dot{Q} .$$

If it is now assumed that no other quantities are pressure dependent and the reaction rate is proportional to pressure to some power, n', then

$$\dot{m} \propto p^{n'/2}$$

Since $\dot{m} = b\, p^n$ describes the deflagration rates fairly well over moderate ranges of pressure, then the n's of Figure 1 should approximately represent one-half the reaction order. On this basis, for the pressures considered in the kinetic analysis, AP, HAP and HDP are close to first-order overall and HP and HNF are second-order.

The foregoing analysis of the burning rates is well known to be an insensitive method of determining reaction kinetics. We have made a parametric analysis of equation (13), which shows the following. If the pre-exponential factors for first and second order were a factor of 10 less than the values chosen, E would be reduced by 3 to 5 kcal/mole. Similarly, if $Q_{c\phi}$ is chosen such as to make L an order of magnitude larger, E is increased by roughly 5 kcal/mole at low E and less at high E. The activation energy is quite insensitive to T_s, a 50° reduction for example reduces E by less than 1 kcal/mole. It is nevertheless of interest to compare the activation energies with some

experimental values found in the literature. The decomposition of perchloric acid vapor (21) occurs with an activation energy of 45 kcal/mole. The calculated values in Table V definitely indicate that this reaction cannot be controlling the deflagration of AP or HAP. The fact that $HClO_4$ decomposition is first-order whereas HP deflagration seems to be second order suggests that it does not control this deflagration either. (However, the calculated second-order activation energy for HP is unreasonable.) Allowing for the uncertainty in the calculations, it does seem possible that HDP deflagration could be controlled by $HClO_4$ decomposition.

It is also relevant to ask whether the burning rates of the hydrazine-based oxidizers could be controlled by the decomposition of N_2H_4. The decomposition rate is known to be faster than the oxidation rate for hydrazine if the oxidant is O_2, and vice versa if the oxidant is NO_2; reaction with $HClO_4$ has not been studied. Actually the chemistry of the HNF system has been elucidated (5) and it was determined that direct attack by NO_2 in a bimolecular oxidation reaction governs the deflagration. Knowing that hydrazine decomposition is first order with E = 54 kcal/mole, one would definitely rule out this reaction as controlling. Hydrazine decomposition does not appear to have a major role in HP deflagration either, based on the calculations in Table V. Finally, it can be concluded that N_2H_4 decomposition probably does not control HDP deflagration whereas $HClO_4$ decomposition possibly does, even though N_2H_4 is the slower of the two. When $HClO_4$ decomposes, very likely its reactive intermediate products would attack N_2H_4, causing rapid reaction. This would leave the perchloric acid decomposition as the slow step in such a sequence.

III. THE EXTINGUISHMENT OF SOLID PROPELLANTS BY RAPID DEPRESSURIZATION

A. DESCRIPTION OF APPARATUS AND TECHNIQUE

An experimental research study was undertaken with the objective of generating data that would be in a suitable form to provide a proper test of extinguishment theories. Data reported in the literature from motor firings, while often of practical value, do not seem to provide the necessary dP/dt - P history throughout the transient or at the moment of extinction. Additionally, in motor tests there are the superimposed effects of erosive burning, the pressure being determined by grain ablation as well as venting, and the possibility of reignition. To overcome these disadvantages an optical strand burner was modified for use as a laboratory-scale apparatus to study extinguishment by rapid depressurization. Other advantages of this type of apparatus are that studies can be conveniently carried out on small strand-size samples of propellant and high-speed motion pictures can be taken of the extinguishment event. A photograph of the disassembled equipment is shown in Figure 8. On the right is the bomb body which has an internal volume of about 300 cc and contains inlet and outlet connections for gas pressurizing and purging. Fused silica windows are provided for taking motion pictures and for monitoring the propellant flame luminosity with a phototube. A #6365 Dumont Multiplier Phototube is used which has an S-11 spectral response. Also mounted in the body in a plane with the propellant surface is a Kistler pressure transducer.

On the left of the photo is shown the bomb head which has a 1-1/4" hole drilled straight through the top. This vent is sealed with a stainless steel frangible diaphragm which, together with an orifice plate to control the depressurization rate, is inserted under the screw cap on top. A diaphragm in a set of retaining rings and three orifice inserts are shown at the bottom of the photo. The head also contains ignition leads and posts to support the stage on which strands are mounted. Attached to the top of the head is a solenoid-driven plunger for rupturing the diaphragm.

A run is carried out by pressurizing the bomb and igniting a strand (leached to prevent side burning). After steady combustion is attained, the

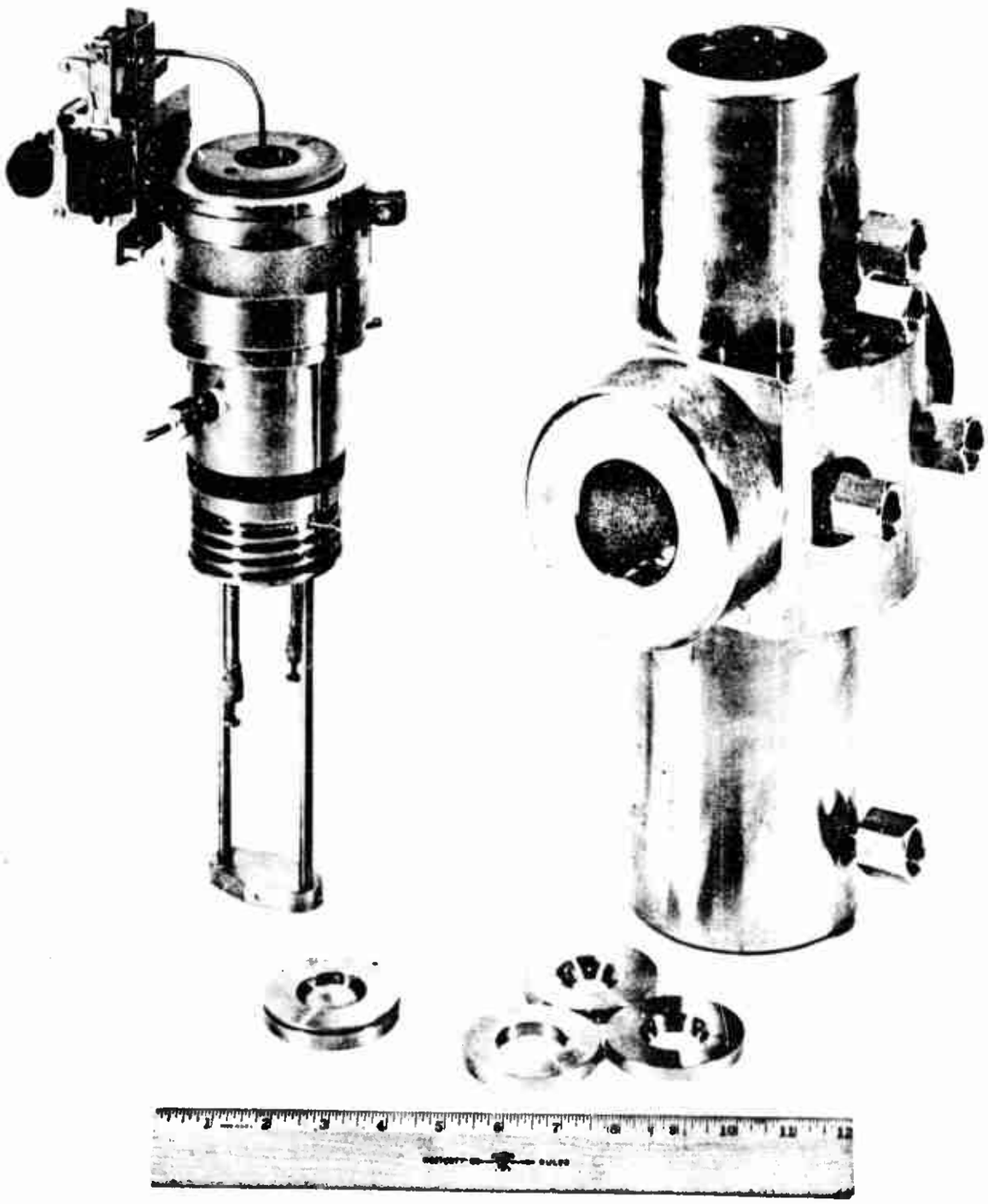

15565

Figure 8. Photograph of Modified Optical Bomb for Study of Extinguishment of Solid-Propellant Strands by Rapid Depressurization. (Discussed in text.)

electrically-timed puncture of the diaphragm is effected and simultaneously a dual-trace oscilloscope is triggered. The outputs of the phototube and pressure transducer are fed into the scope which records the luminosity and pressure decay with time. A Polaroid photograph of a typical oscilloscope display is shown in Figure 9.

The oscilloscope display photos are analyzed by measuring tangents to the pressure-time curve at a number of points along the line using an optically flat piece of half-silvered glass. The instantaneous (-dP/dt)-values are then computed and from a plot of these versus pressure the critical extinction (-dP/dt - P)-point (luminosity zero) is determined. The apparatus can be used at pressures as high as at least 2000 psi with corresponding pressure decay rates of 5×10^5 psi/sec. At present there are only provisions for venting to ambient pressure.

B. RESULTS AND COMPARISON TO THEORY

Extinguishment studies were carried out on three candidate composite propellants. The first, designated Arcite, was a non-aluminized, polyvinyl-chloride-based composite containing 10 percent dioctyl adipate plasticizer and approximately 80 percent bimodal AP. There was a trace of carbon black but no burning rate catalyst. The second, designated PBAA, was a simple polybutadiene-acrylic acid copolymer propellant with no additives. It contained 25.7 percent PBAA, 4.3 percent EPON 828 curative, and 70.0 percent unimodal AP of nominal 80 micron particle size. The third, designated PBAA-Al, was essentially the same as the second except it contained 5.0 percent powdered aluminum of approximately 20 micron particle size. This propellant had 21.4% PBAA, 3.6% EPON 828, and 70.0% AP. Burning rates were measured over the pressure range of interest and are listed below where the values of b and n refer to the equation

$$r_o = b\, P^n$$

where r_o is the steady-state linear burning rate in in/sec when P is in psia.

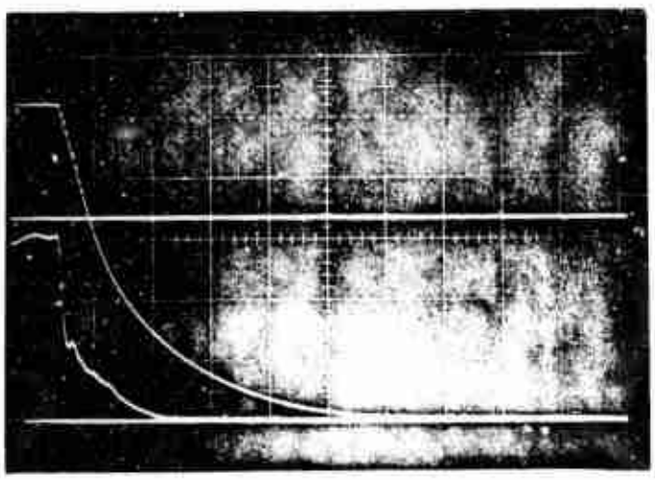

15564

Figure 9. Polaroid Photo of Typical Oscilloscope Display (Arcite Run No. 14). Upper Trace is Pressure Decay from Initial Pressure of 129 psia. Lower Trace is Propellant Flame Luminosity Measured with Phototube. Horizontal Lines are Pressure Calibrations of 15 and 73 psig. Sweep Time is 5 msec/division.

Propellant	b	n
Arcite	0.0128	0.567
PBAA	0.00778	0.498
PBAA-Al	0.01835	0.418

The Arcite propellant burns at least twice as fast as the PBAA at all pressures encountered in the study. Since the theoretical critical pressure decay rate for extinction, $-d(\ln P)/dt$, is proportional to r_o^2 (see below), the two propellants should differ by a factor of four in their extinguishment criteria. (This is slightly reduced by the differences in the n's.)

A total of 47 useful runs were carried out on the three propellants: 14 on Arcite, 18 on PBAA, and 15 on PBAA-Al. Thirty-seven resulted in extinguishment and in 10 runs the depressurization rate was too low to cause extinction. The initial pressures varied from 67.5 to 487 psia. In general what was attempted was to select a nominal initial pressure and then carry out several runs at this pressure in which the depressurization rate was varied. Then a higher or lower pressure was taken, and so on. In this way, fairly good coverage of pressures and (dP/dt)'s was obtained. A summary of pertinent data is given in Tables VI, VII and VIII. In these tables, P_i is the initial pressure; P_e is the pressure at which extinction occurred which was read directly off the oscilloscope records; $-dP/dt$ is the rate of pressure decay at P_e, the instant of extinction; and the columns listed r_o will be discussed below.

We have taken Fastax movies of two extinguishment runs at approximately 3000 frames/sec. In one of these we failed to obtain an oscilloscope record although the movie and run otherwise were normal. The second, Arcite run #14, was satisfactory and the movie provided confirmation that the phototube was properly monitoring the extinction event. On Figure 9 it can be seen that the luminosity reaches zero at 8.8 milliseconds after the pressure begins to decay. In the movie, the arrival of the expansion wave at the flame front is very apparent and the light intensity was no longer visible 8.7 $\pm$0.2 milliseconds later.

The results must be discussed in relation to theoretical concepts of propellant combustion and extinguishment. Several theories of extinguish-

TABLE VI

Experimental Extinguishment Data for Arcite Propellant

Run	P_i (psia)	P_e (psia)	$-\frac{dP}{dt}$ ($\frac{psi}{sec}$) $\times 10^{-3}$	r_{oe} (Theory)	r_o ($\frac{in}{sec}$) (Exper.)
1	425	no extinguishment			
2	430	81	7.7	.12	.16
3	425	71	6.4	.12	.147
4	102	25	1.55	.12	.08
5	99	31.7	2.88	.14	.095
6	105	34	2.41	.13	.098
7	103	no extinguishment			
8	223	35	1.39	.095	.10
9	212	31	0.49	.06	.090
10	214	no extinguishment			
11	67.5	no extinguishment			
12	71	30.6	2.08	.125	.090
13	76	21	0.40	.066	.075
14	129	40.2	3.45	.14	.105

TABLE VII

Experimental Extinguishment Data for PBAA Propellant

Run	P_i (psia)	P_e (psia)	$-\frac{dP}{dt} \times 10^{-3}$ (psi/sec)
1	102	35.6	3.00
2	98	37.1	3.30
3	101	24.2	0.55
4	201	39.8	1.01
5	203	55.3	4.5
6	298	90.	7.5
7	303	48.0	0.77
8	304	97.	12.5
9	199	33.2	0.30
10	109	28.7	0.29
11	262	27.6	0.193
12	388	27.2	0.180
13	97.5	19.8	0.0064
14	106	20.8	0.00225
15	470	25.3	0.00208
16	192	22.7	0.00110
17	179	no extinguishment	
18	375	no extinguishment	

TABLE VIII

Experimental Extinguishment Data for PBAA-Al Propellant

Run	P_i (psia)	P_e (psia)	$-dP/dt \times 10^{-3}$ (psi/sec)
1	107	21.6	0.184
2	201	19	0.131
3	224	24.5	0.148
4	487	27.8	0.153
5	202	36.5	0.79
6	203	59.3	7.30
7	403	83	10.4
8	90	18.7	0.0053
9	479	no extinguishment	
10	379	no extinguishment	
11	203	no extinguishment	
12	275	no extinguishment	
13	106	29.3	2.72
14	298	21.5	0.264
15	480	15	0.178

ment have been presented (13, 22-26), and in this report we shall not review these theories, but only note that there is substantial agreement among those (13, 22, 26) that yield dimensional transient burning rate expressions. The discussion is limited to a comparison of the experimental results with the predictions of the theory of reference 13.

According to reference 13, the linear ablation rate of a solid propellant grain during a pressure transient (decrease) is given by

$$r = b P^n \left(1 + \frac{2\alpha n}{b^2} P^{-(2n+1)} \frac{dP}{dt} \right) \qquad (15)$$

where $\alpha = \lambda/\rho C_p$ is the thermal diffusivity of the solid and $b P^n = r_o$ is the steady-state burning rate. Extinction occurs when $r = 0$, so that

$$-\frac{dP}{dt} = \frac{(b P^n)^2}{2\alpha n} P = \frac{r_o^2}{2\alpha n} P \qquad (16)$$

A log-log plot of dP/dt vs. P will yield a straight line which defines the theoretical extinction boundary. Equation (16) is plotted in Figures 10, 11 and 12 using the measured steady-state burning rates for the propellants of this study and taking $\alpha = .00020$ in^2/sec in every case, which is the approximate average thermal diffusivity for these materials. The points in the figures are the experimental data of the preceding tables. In Figure 10, an actual experimental curve is shown along which extinction occurred. On each figure is shown a typical experimental curve in which no extinction occurred; the no-extinction curves that are not shown all lie in the vicinity of those selected for the figures.

An equivalent rough test of equation (16) can be made by computing r_o's from

$$r_o = \sqrt{2\alpha n \frac{d(\ln P)}{dt}}$$

and comparing with the measured steady-state values at P_e. These are shown for the Arcite propellant in the last two columns of Table VI; the agreement is comparable to that displayed in Figure 10.

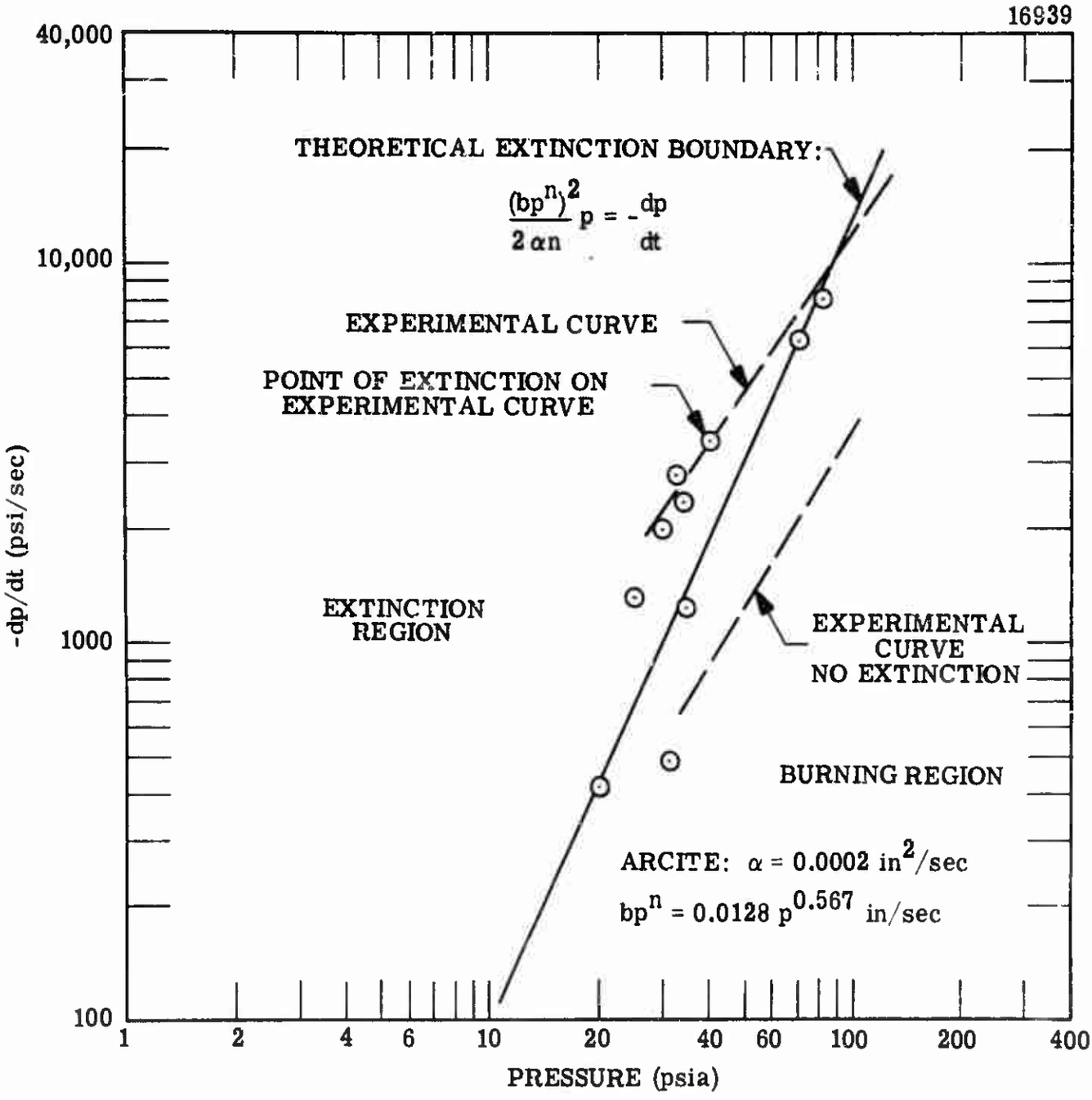

Figure 10. Comparison of Experimental Extinguishment Results for an Arcite Propellant with Theory of Reference 13.

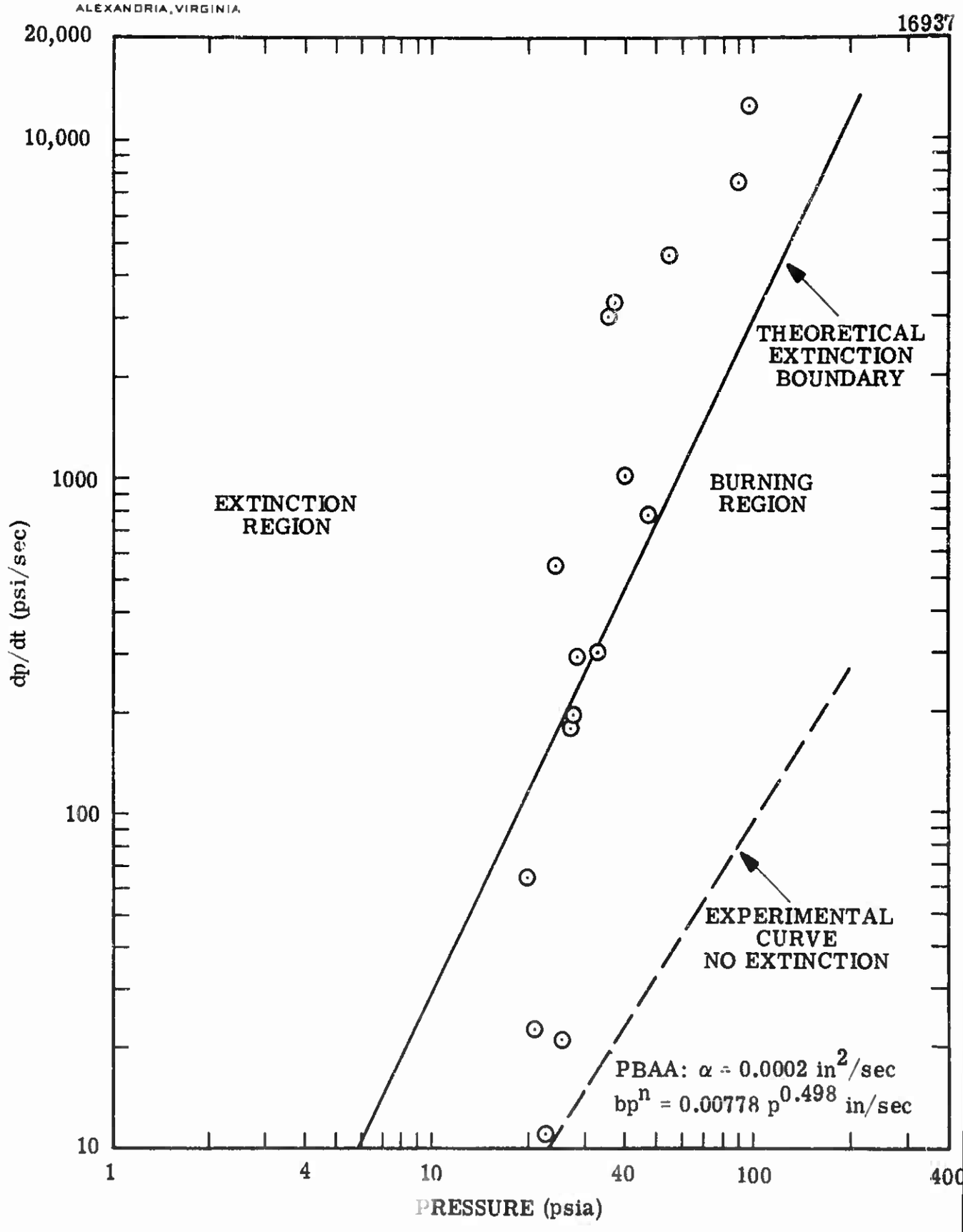

Figure 11. Comparison of Experimental Extinguishment Results for PBAA Propellant with Theory of Reference 13.

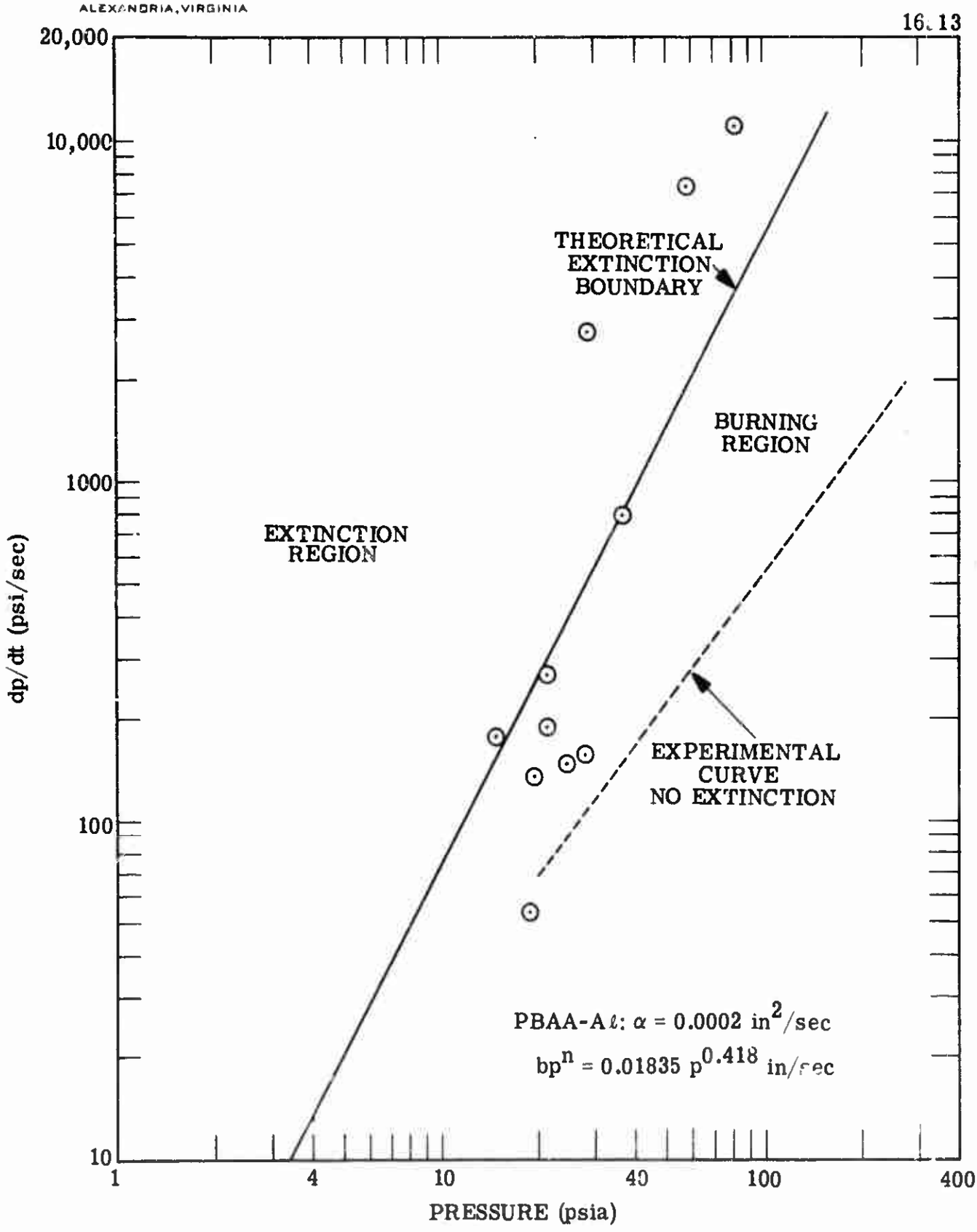

Figure 12. Comparison of Experimental Extinguishment Results for PBAA-Aℓ Propellant with Theory of Reference 13.

We must now evaluate the comparisons of theory and experiment shown in the figures. The theory is based on the change in preheat stored in a propellant grain with change in burning rate. It is essentially a "thermal" theory and the assumptions in it are discussed in reference 13. It was advanced as a useful concept which should be valid to a first approximation in predicting the extinction criteria for solid propellants. From this point of view the agreement between experiment and theory must be judged remarkably good, and can be taken as mutually supporting evidence for the general validity of both. It does appear however that the agreement of the theory with the data of PBAA and the aluminized PBAA could be better. The data show high scatter, but nevertheless in the highest and lowest dP/dt regions the experimental points fall consistently above and below, respectively, the theoretical extinction line. Examining the worst case, for example, PBAA at ∿20 psia extinguishes at a dP/dt that is an order of magnitude less than the theoretical depressurization rate for extinction. Or, alternatively, for this propellant at this extreme condition, the theory misses predicting the pressure at which extinction occurs by a factor of three. This disagreement is not serious enough to invalidate the theory as a good first-order approximation to extinguishment criteria.

IV. REFERENCES

1. Atlantic Research Corporation, "Research on the Deflagration of High-Energy Solid Oxidizers," Final Technical Report, Contract No. AF 49 (638)-1169, November 30, 1965.

2. Friedman, R., Nugent, R. G., Rumbel, K. E., and Scurlock, A. C., Sixth Symposium (International) on Combustion, p. 612, Reinhold Publishing Corporation, New York, 1957; and Levy, J. B. and Friedman, R., Seventh Symposium (International) on Combustion, p. 663, The Williams and Wilkins Co., Baltimore, Md., 1962.

3. Levy, J. B., von Elbe, G., Friedman, R., Wallin, T., and Adams, S. J., Advances in Chemistry Series, No. 54, p. 55, American Chemical Society, Washington, D. C. 1966.

4. McHale, E. T., Adams, S. J., von Elbe, G., and Levy, J. B., Combustion and Flame 11, 141 (1967).

5. Atlantic Research Corporation, "Research on Combustion in Solid Rocket Propellants," Final Technical Report, Contract No. DA-36-034-AMC-0091R, July 21, 1964.

6. Thiokol Chemical Corporation, Elkton Division, "Hydroxylammonium Perchlorate Propellant Research," Final Report G154-63, Contract NOnr 63-0284-C, Sept. 30, 1963.

7. Grelecki, C. J. and Cruice, W., Advances in Chemistry Series, No. 54, p. 73, American Chemical Society, Washington, D. C., 1966.

8. Atlantic Research Corporation, "Research on Solid-Propellant Combustion," Final Technical Report, Contract No. AF 49(638)-813, Dec. 31, 1961.

9. Rosser, W. A., Inami, S. H., and Wise, H., AIAA J. 4, 663 (1966).

10. Fristrom, R. M. and Westenberg, A. A., Flame Structure, McGraw-Hill Book Co., New York, N. Y., 1965, p. 27.

11. Horton, M. D., and Price, E. W., ARS J. 32, 1745 (1962).

12. Hightower, J. D. and Price, E. W., Eleventh Symposium (International) on Combustion, p. 463, The Combustion Institute, Pittsburgh, Pa., 1967.

13. von Elbe, G., "Solid Propellant Ignition and Response of Combustion to Pressure Transients," AIAA Paper No. 66-668, June 13-17, 1966.

14. Lewis, B., and von Elbe, G., Combustion, Flames and Explosions of Gases, 2nd Edition, Academic Press Inc., New York, N. Y., 1961.

15. Hightower, J. D. and Price, E. W., "Two-Dimensional Experimental Studies of the Combustion Zone of Composite Propellants," ICRPG 2nd Combustion Conference, Vol. I, p. 421, May 1966.

16. Markstein, G. H. and Somers, L. M., Fourth Symposium (International) on Combustion, p. 527, Williams and Wilkins Co., Baltimore, Md., 1953.

17. Powling, J., Eleventh Symposium (International) on Combustion, p.447 The Combustion Institute, Pittsburgh, Pa., 1967.

18. Beckstead, M. W. and Hightower, J. D., "On the Surface Temperature of Deflagrating Ammonium Perchlorate Crystals," AIAA Paper 67-68, Jan. 1967.

19. von Elbe, G. and McHale, E. T., "Gasification by Sublimation, Nucleate Boiling and Chemical Attack in Oxidizer Deflagration Waves," ICRPG 2nd Combustion Conference, Vol. I, p. 417, May 1966.

20. Inami, H. S., Rosser, W. H., and Wise, H., J. Phys. Chem., 67, 1077 (1963).

21. Levy, J. B., J. Phys. Chem., 66, 1092 (1962).

22. Paul, B. E., Lovine, R. L., and Fong, L. Y., "A Ballistic Explanation of the Ignition Pressure Peak," AIAA Preprint 64-121, AIAA 5th Solid Propellant Rocket Conference, Palo Alto, California, January 1964.

23. Marxman, G. A., "Theoretical Model of Solid Propellant Response in Combustion Instability and Extinction," ICRPG 3rd Combustion Conference, Cocoa Beach, Fla., Oct. 1966 (CPIA Publication No. 138, Vol. I, Feb. 1967), p. 221.

24. Cohen, N. S., "A Theory of Solid Propellant Extinguishment by Pressure Perturbation," ICRPG 2nd Combustion Conference, Los Angeles, California, Nov. 1965 (CPIA Publication No. 105, Vol. I, May 1966), p. 677.

25. Horton, M. D., Bruno, P. S., and Graesser, E. C., "Depressurization Induced Extinction of Burning Solid Propellant," ICRPG/AIAA 2nd Solid Propellant Conference, Anaheim, Calif., June 1967, p. 232.

26. Krier, H., T'ien, J. S., Sirignano, W. A., and Summerfield, M., "Non-Steady Burning Phenomena of Solid Propellants: Theory and Experiments," ICRPG/AIAA 2nd Solid Propellant Conference, Anaheim, Calif., June 1967, p. 232.

ATLANTIC RESEARCH CORPORATION
ALEXANDRIA, VIRGINIA

APPENDIX

THE EXPLOSIVE DECOMPOSITION OF CHLORINE DIOXIDE

ATLANTIC RESEARCH CORPORATION
ALEXANDRIA, VIRGINIA

THE EXPLOSIVE DECOMPOSITION OF CHLORINE DIOXIDE

A. INTRODUCTION

The known stable oxides of chlorine are chlorine monoxide, Cl_2O; chlorine dioxide, ClO_2; chlorine hexoxide, Cl_2O_6 (which exists as ClO_3 in the vapor phase); and chlorine heptoxide, Cl_2O_7; in addition a fifth compound of empirical formula $ClO_{1.5}$, probably the sesquioxide, Cl_2O_3, has been discovered in the course of this study.[1] The free-radical species ClO is known to exist[2] and the peroxy radical ClOO probably also exists.[2,3,4] This class of compounds has been the subject of considerable research over the past decades, and many publications have appeared dealing with their reactions and slow and explosive decomposition. The striking feature of all the work on the kinetics of these compounds is that no mechanisms have been proposed which account for the thermal decomposition of the stable compounds. The principal reason for this, in the case of the two simplest of the stable oxides, Cl_2O and ClO_2, is that the explosive decompositions are of a degenerate chain-branching type. Delayed explosions such as these are due to the buildup of an intermediate, which gives rise to a branched-chain reaction. The intermediates have not been identified, and hence it was not possible to postulate a decomposition mechanism, even though accurate rate data were available.

Another impediment to understanding what elementary reactions have an important role in chlorine oxides kinetics was an erroneous value for the heat of formation of the ClO radical. Thus an extensive discussion of such reactions by Szabo[5] is no longer relevant, since he based his arguments entirely on a value of 37 kcal/mole, whereas more recent spectroscopic data have established ΔH_f°(298°K) for ClO as 24.2 kcal/mole.[6]

We report here a study of the explosive decomposition of ClO_2 in the range 54 to 134°C and 0.2 to 40 Torr. Experiments were performed on the induction time to explosion as a function of pressure and temperature, the effect of vessel size and added gases, and the effect of addition of other chlorine oxides. The intermediate responsible for degenerate chain-branching

has been identified as Cl_2O_3. The results of the present study together with those of Schumacher and Stieger[7] on the thermal decomposition, and present reliable enthalpy data on the chlorine oxides, allow us to write a mechanism which can successfully account for the behavior of ClO_2 over a wide range of conditions.

B. EXPERIMENTAL

Chemicals: Chlorine dioxide was synthesized as needed by mixing $KClO_3$ with moist oxalic acid and warming to about 90°C:

$$2KClO_3 + 2H_2C_2O_4 \xrightarrow[\Delta]{H_2O} K_2C_2O_4 + 2H_2O + 2CO_2 + 2ClO_2$$

The reaction was carried out at atmospheric pressure under a stream of N_2. The ClO_2 was passed through Drierite and Ascarite, which removed most of the H_2O and CO_2, after which it was collected at -196°C and finally fractionated and stored under vacuum at -78°C. Purity was checked by measuring the vapor pressure[8] and infrared spectrum.[9] No impurities were ever found, and we estimate the purity as at least within a few tenths of a percent of one hundred. Preparations and handling operations were all carried out in darkness.

The chlorine heptoxide used in some of the experiments was synthesized by dehydrating $HClO_4$ (72%) with excess P_2O_5 by the method reported by Goodeve and Powney.[10] Its vapor pressure was checked against the literature value.[10]

The preparation of chlorine hexoxide and chlorine sesquioxide for use in this study has been reported.[1] Essentially the method consists of irradiating ClO_2 at -45°C, and, upon completion, pumping away the Cl_2 and O_2 products. The remaining products, Cl_2O_6 and Cl_2O_3, can be added to ClO_2 selectively as required because of the difference in their volatility. The purified Cl_2O_6 has approximately one Torr vapor pressure at 25°C,[11] and this correspondence to the reported value was taken as indicative of high purity since all the other chlorine oxides have very high vapor pressures.

The N_2, O_2, Cl_2, and He were standard high-purity gases which are commercially available.

Apparatus: A standard apparatus for studying gas explosions was used. This was constructed entirely of Pyrex and resembled in many of its essentials that described by Kaufman and Gerri,[12] who verified its applicability for this type of study. It consisted of a 100- or 200-cc spherical explosion bulb connected by 8 mm i.d. tubing and an 8 mm bore straight-through stopcock to a vacuum system. The explosion bulb was immersed in a glycerol bath, the temperature of which was controlled (±0.1°C) by an American Instrument Company Bimetal Thermoregulator. This controlled a relay which in turn activated an immersion heater.

The vacuum system consisted of storage bulbs, traps, and a mercury manometer. A vacuum of <0.1 Torr could be attained with a mechanical pump. All stopcocks were lubricated with Kel-F grease and the mercury was covered with a layer of Kel-F oil. No problems of attack by the chlorine oxides on the grease or oil were encountered. The ClO_2 synthesis train was connected to the vacuum system.

The characteristic parameter that was measured in this study was the induction time to explosion. Since this time was of the order of seconds to minutes it could be measured by a stopwatch. The procedure consisted of admitting the ClO_2 from a reservoir bulb (covered with a black cloth bag) to the explosion bulb by turning the straight-through stopcock. The pressure was measured in the vacuum manifold after admission and this was taken to be the pressure in the explosion bulb. Preliminary experiments showed that approximately 98% of the manifold pressure was realized in the bulb. The time from admission to explosion, as evidenced by a flash of white light, was measured. Heating times at the highest densities of this study were estimated from reference 12 to be of the order of tens of milliseconds.

C. RESULTS

General Remarks on the Reaction

Explosions with pure chlorine dioxide have been obtained at all working temperatures from 54 to 134°C. There is a lower temperature limit, which

is at approximately 45°C. At this temperature, Schumacher and Stieger[7] have occasionally observed spontaneous explosions. In our work we have always had explosions at 54°C, but at 30°C we have not observed spontaneous explosions even with 50 Torr ClO_2 which stood for as long as four days, finally being consumed by slow decomposition. Pressure limits were not observed, and explosions were obtained at all working pressures from approximately 0.2 Torr (above 60°C) to 40 Torr. Induction periods varied from 3 seconds to 18 minutes depending on temperature and pressure, but were most sensitive to vessel walls. It was found, for example, that if ClO_2 was even allowed to remain in the reservoir bulbs in complete darkness at ambient temperature prior to explosion for varying lengths of time, the induction periods were so drastically affected as to give rise to large errors in general trends of results. Data obtained from ClO_2 expanded from 1-liter storage bulbs differed markedly from those from 0.5-liter bulbs. Accordingly, to compare data from different sets of experiments it was necessary to insure that such effects were being carefully controlled. Likewise, light has a tremendous sensitizing effect on the reaction and similar precautions had to be taken.

Typical variation of induction-time-to-explosion with initial ClO_2 pressure is as shown by the curve of Figure 1. At high pressure the induction time becomes independent of the initial ClO_2 concentration; and at low pressure it becomes a very sensitive function of it. Similar hyperbola-type curves were obtained over the whole temperature range studied. All the data presented below were obtained in a 200-cc spherical explosion bulb, except those of Figure 2.

Effect of Added Gases

In Figure 1 also is shown the effect of added nitrogen on the induction times. The ordinate refers to the partial pressure of ClO_2 only. We have obtained the same type of curves with added O_2, Cl_2, and He, which are all but indistinguishable from that shown for N_2. Neither have we found any difference in the effect over the temperature range 58 to 76°C. The greater the amount of added inert gas, the greater the shortening of the induction time. The most significant property of the promoting effect of added gases is that it is constant over the entire pressure range. Greater or less promotion was

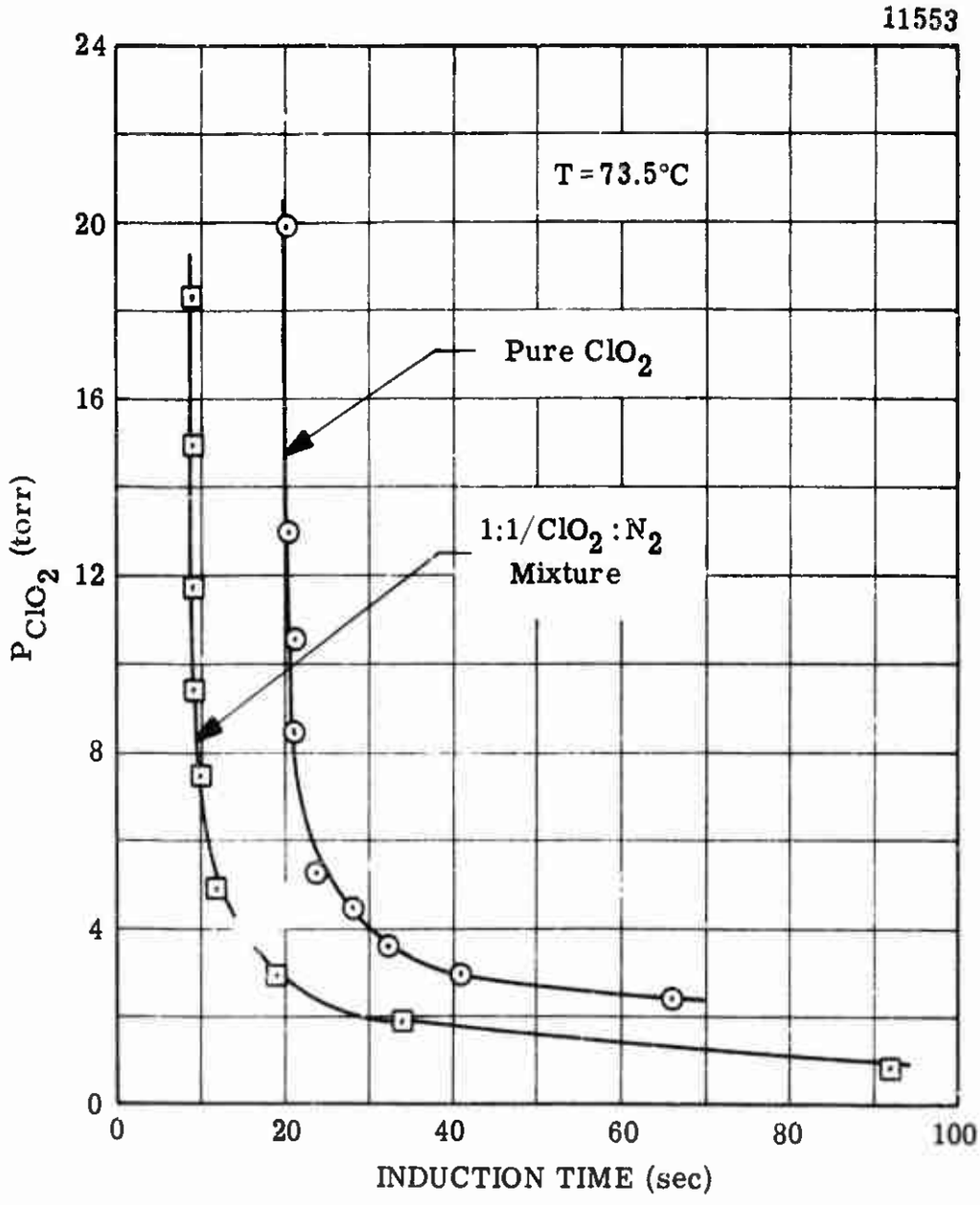

Figure 1. Typical Curve of Induction Time for ClO_2 Explosion Versus Initial Pressure, Showing also the Effect of Added N_2.

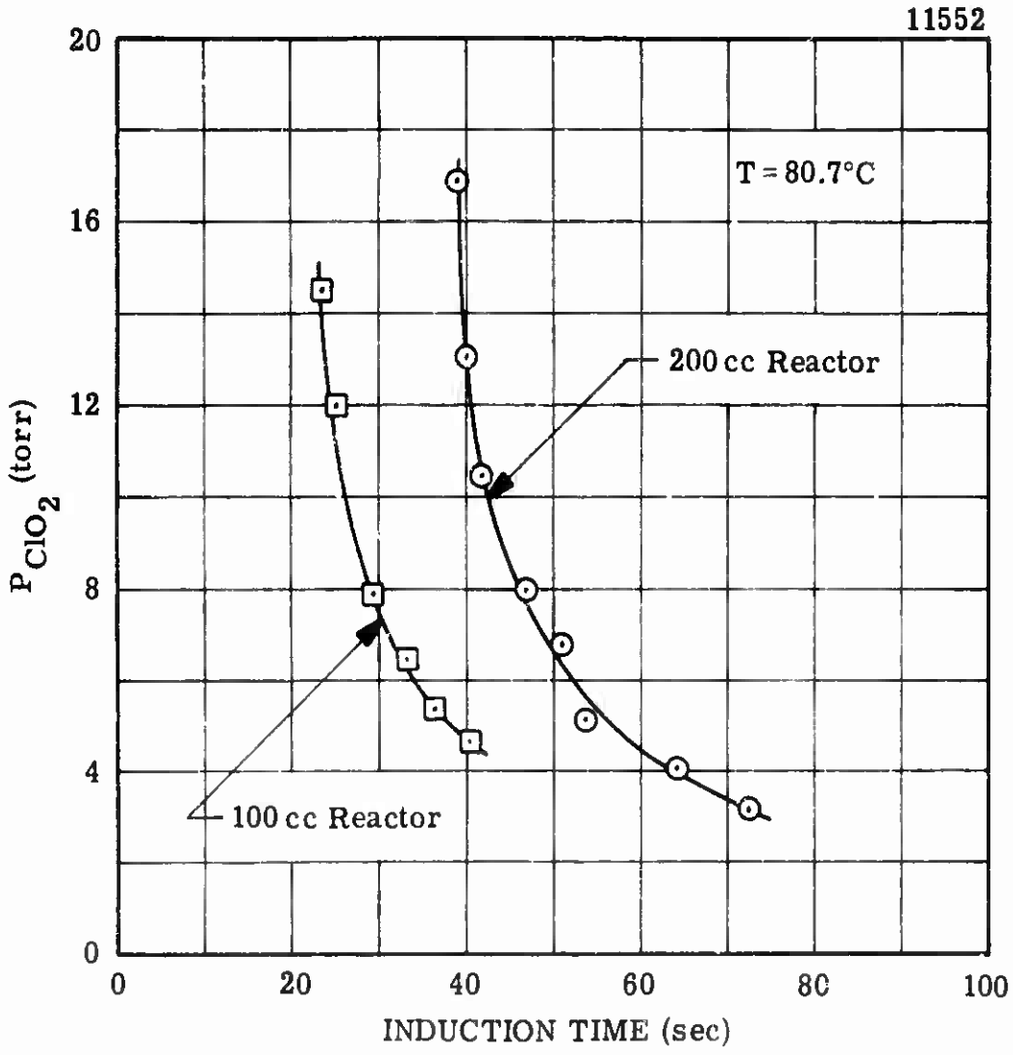

Figure 2. Induction Periods for ClO_2 Explosions in Two Different Size Spherical Pyrex Vessels.

not observed at high or low pressure over a range of almost two ordera of magnitude. The added-gas promotion effect is therefore assigned to the impeding of diffusion of radicals to the vessel walls where chain termination can occur. It is not at all consistent with promotion of three-body propagation reactions, since this would require the promotion effect to diminish with decreasing pressure, the frequency of termolecular to bimclecular colliaions being inversely proportional to pressure.

Effect of Varying Surface Area to Volume Ratio

Exploaions in 100- and 200-cc apherical Pyrex bulbs were made and the results are shown in Figure 2. The variation in A/V ratio was 1.26; the induction timea in the smaller reactor were shorter by approximately a factor of 0.6. This ia strong evidence that chain initiation occurs on the wall, as Schumacher and Stieger[7] report for their experimenta at 45°C. The conclusion is not unequivocal, since, as mentioned, reproducibility of aurfacea waa difficult to obtain. However, repeated experimenta indicated that the surfaces of the two bulbs were of equal activity.

Another observation which bears on the matter of surface reactions is the following. We have attempted to stream ClO_2 highly diluted with N_2 at atmospheric pressure through an 8 mm i.d. U tube maintained at 100°C. In every case the ClO_2 exploded as soon as it reached the U-tube entrance. Packing the tube with glass wool prevented explosion and ClO_2 could be passed through indefinitely. Thus, while an increase in surface area promotes explosion up to a point, enough surface can prevent it.

Temperature Dependence of the Reaction

The induction periods as a function of temperature, over a concentration range at each temperature approximately as in Figure 1, were determined from 65 to 134°C. A plot of the data at 15 Torr, where the induction times begin to become independent of pressure, is shown in Figure 3. A change in the slope of the line at 90°C is very prominent. The line in the high temperature region is given by the equation (τ in seconds, T in °K):

$$\log \tau = \frac{2,420}{T} - 5.56 \qquad \text{(above 90°C)}$$

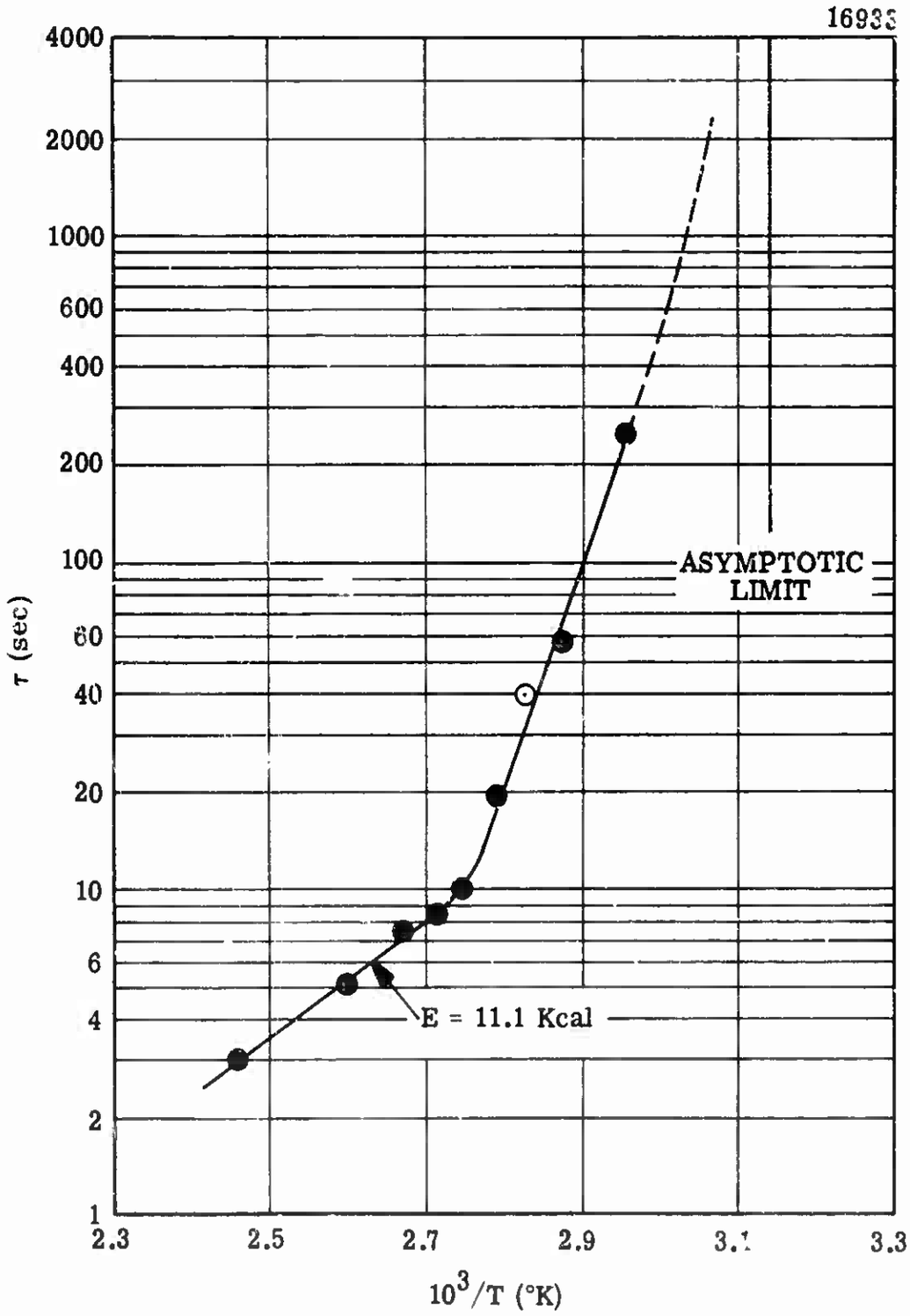

Figure 3. Temperature Dependence of ClO_2 Explosion Induction Periods for 15 Torr Initial Pressure.

We note that if the data of Figures 1 and 4, for example, were plotted on Figure 3, the two resulting points would not fall on the line. This serves to indicate the magnitude of the scatter that is obtained when prior handling and storage of ClO_2 are not controlled, or when reactor surface changes occur. The data of Figure 3 were all obtained in a series of experiments carried out at the same time, and using the same reserve supply of ClO_2, with the exception of the run shown as an open circle which was obtained the following day under identical conditions. The significance of the temperature dependence of τ is considered in the Discussion section.

Effect of Cl_2O_7, ClO_3, and Light

The principal reason for examining the effect of added chlorine oxides on ClO_2 explosions was to determine whether any of these was the intermediate. Cl_2O has been ruled out by Schumacher and Stieger[7] who found that it had a slight inhibiting effect and was consumed in the slow reaction. We have added 2% Cl_2O_7 to ClO_2 and compared induction periods for this mixture with those for pure ClO_2 at 61.2°C. No difference was observed over the pressure range 36 to 4 Torr. Infrared analysis of irradiated ClO_2 (see below) had established that the intermediate in concentrations of <1% would reduce the induction time by approximately an order of magnitude. Hence, Cl_2O_7 was confidently eliminated from further consideration.

Cl_2O_6 is a red oil with ca. 1 Torr vapor pressure at room temperature.[11] The Cl-Cl bond is reported to be 1.75 ±0.5 kcal/mole,[13] and it exists entirely as ClO_3 in the vapor.[11] The approach taken to determine the effect of ClO_3 was to fill a 500-cc reservoir bulb with ClO_2 at a given pressure. The bulb contained a pool of Cl_2O_6 liquid, thus assuring that the ClO_2 always contained 1 Torr ClO_3. Induction periods for this mixture were compared to those for pure ClO_2 and results for 64°C are shown in Figure 4. The percentage ClO_3 in ClO_2 varied for each measurement. Thus the point at 82 sec on the "ClO_3-added" curve represents 1 Torr ClO_3 in 16.5 Torr ClO_2 or 5.7%; the point at 235 sec represents 1 Torr ClO_3 in 7.4 Torr ClO_2 or 11.9%. ClO_3 is seen to have an inhibiting effect and at approximately the 15% level it apparently prevents explosion altogether. This is presumably by the reaction $ClO_3 + ClO \rightarrow 2\ ClO_2$. Chlorine hexoxide (or ClO_3) is known to form in the

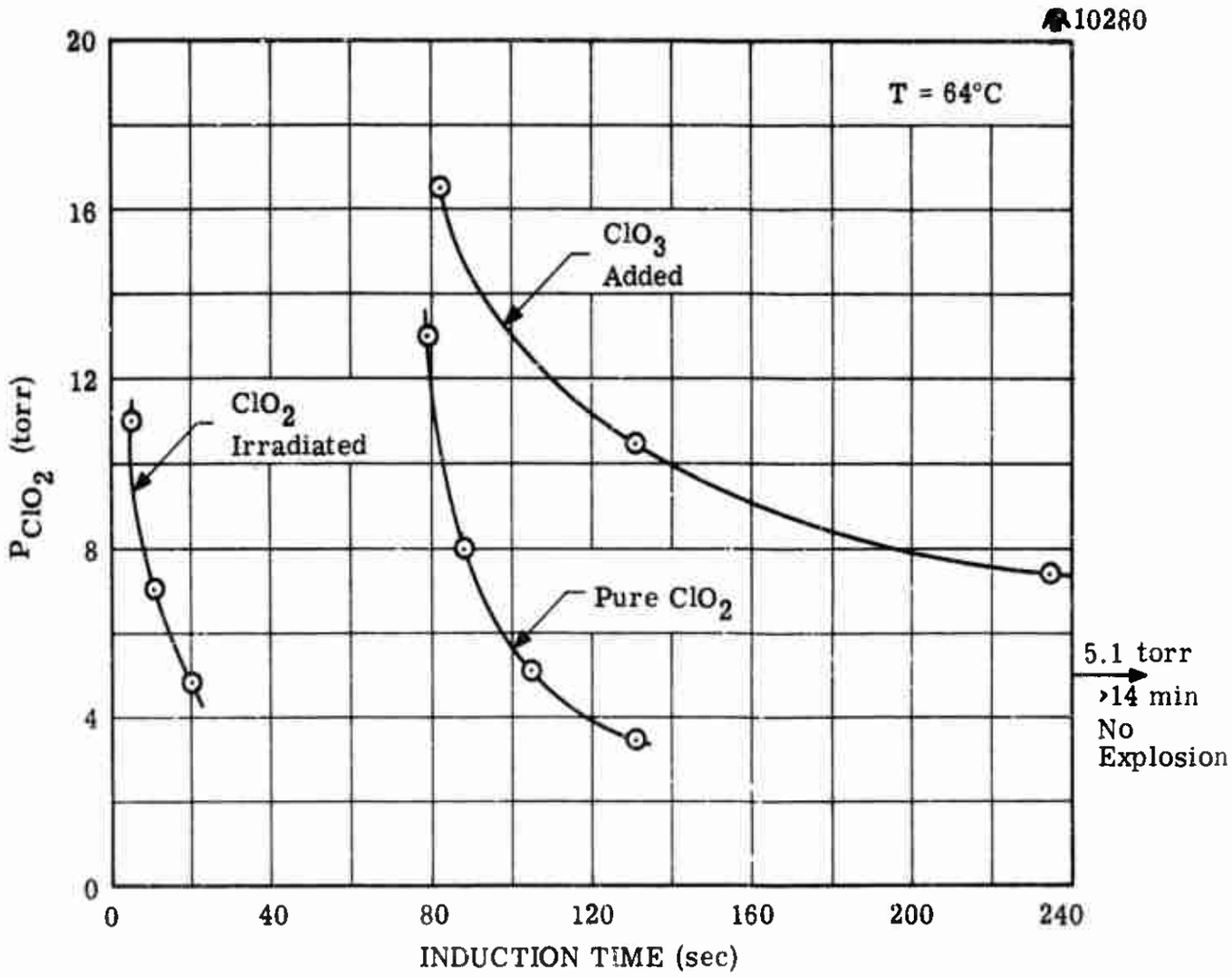

Figure 4. Effect of ClO_3 and Light on Induction Period for ClO_2 Explosions.

decomposition of ClO_2 [14] and has been suspected as being the intermediate which leads to explosion. This work shows this not to be the case.

Chlorine dioxide that has previously been irradiated is very sensitive to explosion. The points on the "ClO_2-irradiated" curve of Figure 4 correspond to pure ClO_2 that was subjected to low-intensity UV light through Pyrex for 2 minutes. The first explosion, at 11 Torr, was made immediately after irradiation. The second point was obtained five minutes later, and the third point after another five-minute delay (no irradiation during the delays). It is clear from the position and shape of the curve that the intermediate, formed in photolysis, is stable in the presence of ClO_2 even upon prolonged standing. The concentration of intermediate that can be produced in this way however is certainly small, since infrared analysis of irradiated ClO_2 failed to show any absorption bands not present in the pure material.

Effect of Cl_2O_3

Since none of the known chlorine oxides is the intermediate in the delayed explosions of ClO_2, but the intermediate can be produced by irradiating ClO_2, albeit in low concentrations, it was decided to photolyze ClO_2 at low temperature in the hope of being able to isolate the intermediate in sufficient quantity to work with it. This approach proved successful and we were able to synthesize and identify a new oxide of chlorine. The details of this phase of the study have been reported previously[1] and only an abbreviated summary will be given here together with a description of the effect of this oxide on the explosion.

When ClO_2 is photolyzed at -45°C, a dark brown solid forms which is a mixture of Cl_2O_6 and Cl_2O_3. The formation of the former compound has been known for a long time;[14] the composition of the latter compound was determined by degrading it to O_2 and Cl_2 and measuring the O_2/Cl_2 ratio. The mixture has essentially zero vapor pressure at -45°C, but upon slight warming, Cl_2O_3 volatilizes readily, while Cl_2O_6 remains non-volatile. This permits a facile separation; however, when Cl_2O_3 is allowed to vaporize in vacuo it explodes when the pressure reaches ca. 1 Torr. When Cl_2O_3 is allowed to vaporize into a ClO_2 atmosphere, by slight warming from -45°C, no explosion occurs. This technique was then used to determine the effect of added Cl_2O_3 on ClO_2 explosion induction times.

The question one would like to answer is: How does the induction time vary with $[Cl_2O_3]/[ClO_2]$ ratio? This variation may depend on temperature and even on pressure. Attempts to get a precise and thorough answer were not wholly successful for the following reasons: The ratio of $[Cl_2O_3]/[ClO_2]$ at explosion is very small, as is the change in this ratio with temperature. Pure ClO_2 upon standing builds up Cl_2O_3, but it also yields ClO_3 which inhibits the explosion. Furthermore, when Cl_2O_3 is added to ClO_2, the former gradually decomposes in significant amounts even during short handling times. These complications led us to estimate the accuracy of the following data as within a factor of 2 to 3.

Various amounts of Cl_2O_3 were added to ClO_2 and experiments were made at 52, 62 and 72°C. Within the experimental uncertainty the quantity of Cl_2O_3 needed to reduce the induction time a given amount did not vary with temperature. Complete invariance with pressure was found, as judged by the congruency of curves with and without Cl_2O_3 added. In the following table are the data at 62°C for four experiments at 15 Torr ClO_2.

Table 1. Effect of Addition of Cl_2O_3 on the Induction Period

$T = 62°C$ $\qquad$ $P_{ClO_2} = 15$ Torr

% Cl_2O_3 Added	Induction Time (Sec)
0	109
0.2	57
2	1
15	Flashback through Stopcock

Thus we conclude that Cl_2O_3 is the intermediate, and in quantities of the order of 0.2% will reduce the induction time by a factor of two. The effect is independent of pressure, and independent of temperature within a factor of 2-3.

D. DISCUSSION OF THE EXPLOSIVE REACTION MECHANISM

The explosion of ClO_2 is of a degenerate chain-branching type involving the formation of a stable intermediate. Systems of this type are referred to by Semenov[15] where he shows that explosions with induction periods exceeding a few seconds cannot be thermal in nature or of the ordinary chain-branching type. They are a special case of the latter in which the reactant forms a stable intermediate. This intermediate gives rise to chain branching, and the delay time is associated with the buildup of this intermediate to a critical concentration. This type of reaction system must follow a general scheme, which must in its essentials resemble the following:

$R \xrightarrow{i}$	$x + \ldots$		initiation
$R + x \xrightarrow{p}$	$I + \ldots$		propagation
$I + x \xrightarrow{b}$	$n\,y + \ldots$		branching
$R + y \xrightarrow{b'}$	$m\,x + \ldots$		branching
$y \xrightarrow{t}$			termination

Here R = reactant; x and y = highly reactive species (radicals); I = stable intermediate; n and m are branching coefficients ≥ 2.

For such a scheme, the steady-state approximation will hold for [x] and [y]. Thus

$$\frac{d[I]}{dt} = k_i[R]\,\frac{k_p[R] - k_b[I]}{k_p[R] - \alpha k_b[I]}$$

where

$$\alpha = \frac{(m \cdot n - 1)\,k_{b'}[R] - k_t}{k_{b'}[R] + k_t}$$

For $\alpha > 1$ the system will explode since the denominator of the rate equation will approach zero faster than the numerator. α will exceed unity when the rate of reaction b' exceeds that of reaction t. When conditions of temperature and pressure do not favor explosion, the steady-state concentration of

intermediate will be

$$[I]_{ss} = \frac{k_p[R]}{k_b} \quad .$$

For explosive conditions

$$[I]_{crit} = \frac{1}{\alpha} \frac{k_p[R]}{k_b} \quad ,$$

hence the system will explode when some fraction, $1/\alpha$, of the steady-state concentration is reached.

To determine the induction time to explosion, the above rate equation is integrated. It is assumed that [R] does not change appreciably during the induction period; the critical conditions (integration limits) are $[I] = 0$ at $t = 0$ and $[I] = [I]_{crit}$ at $t = \tau$. Integration then yields (see equations 2-6 below):

$$\tau = \frac{k_p}{k_i k_b} \cdot \frac{1}{\alpha}$$

A mechanism that one would write for ClO_2 explosion would have to be of the general form of that shown above with variation to account for the observed experimental results, the general features of which we summarize. Chain initiation and termination take place on the vessel walls. These are established by the promotion effects observed when the surface-to-volume ratio is increased and when inert gases are added, respectively. In addition, a homogeneous termination reaction is required by the observation of a lower temperature limit and the absence of pressure limits, as will be shown below. With the exception of Cl_2O_3, none of the other chlorine oxides has an effect of particular relevance for purposes here. Finally, a hyperbola-like dependence of induction time on initial ClO_2 pressure must follow from the mechanism. From the foregoing considerations together with known enthalpy data on the chlorine oxides and with Cl_2O_3 identified as the intermediate, the following mechanism is suggested for ClO_2 decomposition.

We believe the initiation reaction to be

$$2ClO_2 \xrightarrow[wall]{} ClO + ClO_3$$

the heat of which is 11 kcal/mole, based on $H_f°(298°K)$ of 25, 24 and 37 kcal/mole, respectively, for ClO_2, ClO and ClO_3.[6,16] This reaction accounts for the formation of ClO_3 found in the slow and the explosive reaction, and has the virtue of a low reaction heat and possibly a low activation energy. The alternative unimolecular reaction

$$ClO_2 \xrightarrow[w]{} ClO + O$$

has a thermodynamic heat of 57 kcal/mole and might require a high E_{act} even on a surface. The formation of the intermediate is undoubtedly by the association reaction

$$ClO_2 + ClO \rightarrow Cl_2O_3 \quad .$$

The structure of Cl_2O_3 is postulated as

$$\begin{matrix} O \\ \diagdown \\ O \diagup \end{matrix} Cl\text{-}Cl\text{-}O \quad ,$$

the arguments for which are presented in an earlier publication,[1] where the alternative structures O-Cl-O-Cl-O, Cl-O-O-O-Cl, and O-Cl-O-O-Cl are by implication ruled out. The Cl-Cl bond dissociation energy we estimate as a few kcal, based on comparison with $O_3Cl\text{-}ClO_3$ which has a Cl-Cl bond of 1.73 kcal.[13] If the $O_2Cl\text{-}ClO$ bond is 4 kcal, then the heat of formation of Cl_2O_3 is 45 kcal/mole, which value we use in the following discussion. The very weak bond explains why Cl_2O_3 is such a labile molecule in the gas phase even at low temperature but is stabilized by the presence of ClO_2, presumably by the rapid equilibrium

$$ClO_2 + ClO \rightleftarrows Cl_2O_3$$

As the intermediate builds up in concentration, its reaction with the chain carrier ClO becomes increasingly more important. The most reasonable

ways for this reaction to occur are

$$ClO + Cl_2O_3 \rightarrow O_2Cl\text{-}ClO \cdots ClO \rightarrow ClO_2 + ClOClO$$

and

$$O_2Cl\text{-}ClO + ClO \rightarrow O_2Cl\text{-}ClO \cdots OCl \rightarrow ClO_2 + ClOOCl$$

In the first reaction, the ClOClO species could decompose in three ways:

$$ClOClO \xrightarrow{i} Cl_2O + O$$
$$\xrightarrow{ii} ClO_2 + Cl$$
$$\xrightarrow{iii} 2ClO$$

None of these reactions is chain branching or lead to branching, and need not be considered in the explosion mechanism. We therefore choose the second reaction since it readily leads to branching and explosion through Cl-OO-Cl, which is a free-radical-type species similar to Cl-OO. Benson and Buss[3] estimated D(Cl-OO) as 8 kcal. It seems likely that D(Cl-OOCl) will be approximately the same.* Thus, the dissociation reactions

$$ClOOCl \rightarrow Cl + OOCl \rightarrow 2Cl + O_2$$

should be rapid even at 50°C. Once Cl atoms are produced, the branching reaction

$$Cl + ClO_2 \rightarrow 2ClO$$

is expected to occur, which is 6 kcal/mole exothermic.

The choice of the termination reactions which are dominant under the conditions of this study is determined by the observed kinetics. The reactions

$$Cl + ClO_2 \rightarrow Cl_2 + O_2$$

and

---

* This assumption finds support by compsrison with the oxygen-fluorine analogs. D(F-OOF) is thought to be approximately 17 kcal; D(F-OO) is estimated at 15 kcal [J. B. Levy and B. K. W. Copeland, J. Phys. Chem. 69, 408 (1965)]. Hence one would expect the Cl-O bonds in Cl-OO and Cl-OO-Cl to be approximately the same strength as each other. The fact that F_2O_2 is stable (enough to isolate at low temperature) and Cl_2O_2 is not is probably due to the F-O bonds being considerably stronger.

$$Cl \xrightarrow[wall]{} 1/2\ Cl_2$$

serve to adequately describe the system.

The complete mechanism will then be

$$2ClO_2 \overset{a}{\underset{w}{\rightleftarrows}} ClO + ClO_3$$

$$ClO + ClO_2 \xrightarrow{1} Cl_2O_3 \qquad \Delta H \doteq -4 \text{ kcal}$$

$$ClO + Cl_2O_3 \xrightarrow{2} ClO_2 + ClOOCl \qquad \Delta H \doteq -2 \text{ kcal}$$

$$ClOOCl \xrightarrow{3} ClOO + Cl \qquad \Delta H \doteq +8 \text{ kcal}$$

$$ClOO \xrightarrow{4} Cl + O_2 \qquad \Delta H \doteq +8 \text{ kcal}$$

$$Cl + ClO_2 \xrightarrow{5} 2\ ClO \qquad \Delta H = -6 \text{ kcal}$$

$$Cl + ClO_2 \xrightarrow{6} Cl_2 + O_2 \qquad \Delta H = -54 \text{ kcal}$$

$$Cl \xrightarrow[w]{7} 1/2\ Cl_2$$

We make the assumption that the concentrations of the species Cl, ClO, Cl_2O_2, and ClOO are in a steady state during the induction period. The rate of accumulation of intermediate, which is not in a steady state, is then given by

$$\frac{d[Cl_2O_3]}{dt} = K_a \frac{k_1[ClO_2] - k_2[Cl_2O_3]}{k_1[ClO_2] - \alpha k_2[Cl_2O_3]} \quad \ldots\ldots \quad (1)$$

where K_a is the rate of reaction a, and

$$\alpha = \frac{(3k_5 - k_6)[ClO_2] - K_7}{(k_5 + k_6)[ClO_2] + K_7}$$, K_7 being

the heterogeneous rate constant.

Examination of equation (1) immediately indicates that, since $[Cl_2O_3]$ starts at zero, $d[Cl_2O_3]/dt$ will go to infinity (mathematically) for $\alpha > 1$, and will go to zero for $\alpha < 1$. Ignoring for the moment reaction 7, α will exceed

unity when the rate of branching or k_5 exceeds the rate of homogeneous termination or k_6. This condition is only a function of temperature, and as mentioned earlier will occur above a temperature of approximately 45°C. Surface termination (K_7) will alter this condition, and by providing enough surface area, such as packing a vessel with glass wool which increases K_7 and keeps $\alpha < 1$, explosion can be prevented even at high temperature, again in agreement with experiment. Also, K_7 is inversely proportional to the total pressure since diffusion of Cl atoms to the wall is impeded by increasing pressure, and added gases would be expected to show a promoting effect.

To determine the ClO_2-pressure dependence of the induction time for comparison with experiment, equation (1) must be integrated. Szabo[17] has shown how this can be done rigorously without a computer by using the corresponding equation for $-d[ClO_2]/dt$ and knowing or estimating the rate constants. This procedure yields exact correspondence with the experimental data, which is not required here since the decomposition has such a strong heterogeneous component. Furthermore, the rate constants are not known and most of them could not be very well estimated. We have used a procedure which is less rigorous but which takes into account the first-order effects. This involves the assumption that ClO_2 concentration remains constant during the induction period. This can be checked by referring to Schumacher's[18] work where it is seen that approximately 50 percent of the ClO_2 decomposes prior to explosion. We are really interested in the change in $[ClO_2]$ relative to the change in $[Cl_2O_3]$, and since the latter changes by orders of magnitude during the induction period, the assumption seems very valid for purposes here.

We integrate equation (1) by writing it as

$$\frac{1}{A}\frac{d\phi}{dt} = \frac{1-\phi}{1-\alpha\phi} \qquad \ldots\ldots \qquad (2)$$

where $\phi = k_2[Cl_2O_3]/k_1[ClO_2]$ and

$A = k_2K_a/k_1[ClO_2]$

Integrating from 0 to ϕ and 0 to t:

$$(\alpha - 1)\log(1-\phi) + \alpha\phi = At \qquad \ldots\ldots \qquad (3)$$

The explosion condition is now $\phi = 1/\alpha$ when $t = \tau$. Hence,

$$(\alpha - 1) \log \left(1 - \frac{1}{\alpha}\right) + 1 = A\tau \qquad \ldots\ldots \qquad (4)$$

Expanding the left-hand side as a power series and reducing,

$$\frac{1}{\alpha}\left[\frac{1}{2} + \frac{1}{6\alpha} + \frac{1}{12\alpha^2} + \cdots + \frac{1}{n(n+1)\alpha^{n-1}}\right] = A\tau \quad \ldots \qquad (5)$$

or $$\tau = \frac{1}{\alpha A} \cdot f(\alpha) \quad , \qquad \ldots \qquad (6)$$

when $f(\alpha)$ contains the series in the brackets of equation (5); $f(\alpha)$ converges for $\alpha > 1$ and becomes infinite for $\alpha < 1$. The values of the series are tabulated for some values of α:

α	<1	1	2	3	∞
$f(\alpha)$	∞	.97	.62	.57	.50

Under explosion conditions, α will be greater than unity but never very much greater. Hence for purposes of determining the dependence of τ on $[ClO_2]$, $f(\alpha)$ can be taken as constant ≈1.

Using equation (6) then as $\tau = 1/\alpha A$ we can determine the dependence of τ on $[ClO_2]$. The rate of the surface initiation reaction, which appears in A, even though written as bimolecular, will be first order in $[ClO_2]$ at low pressure. This reaction will probably occur by a mechanism such as

$$ClO_2 + S \xrightarrow{a'} ClO_2 \cdot S$$

$$ClO_2 \cdot S + ClO_2 \xrightarrow{a''} \text{products}$$

for which at low pressure $\frac{-d[ClO_2]}{dt} = 2\, k_a, [S][ClO_2]$

where S is a reaction site. True bimolecular surface reactions involving a

single reactant species, which for chlorine dioxide would be

$$ClO_2 + ClO_2 + S \rightarrow (ClO_2)_2 \cdot S \rightarrow \text{products},$$

are all but unknown.[19] Hence we write

$$K_a = k_a [ClO_2]$$

The rate constant of reaction 7, which appears in α, will be inversely proportional to total pressure, since it depends on the diffusion coefficient[20] which is inversely proportional to pressure. Total pressure will be approximately equal to ClO_2 initial pressure, hence we write $K_7 = k_7/[ClO_2]$. Making this substitution,

$$\alpha = \frac{(3k_5 - k_6)[ClO_2]^2 - k_7}{(k_5 + k_6)[ClO_2]^2 + k_7} .$$

The induction time now becomes

$$\tau = \frac{k_1}{k_2 k_a} \frac{(k_5 + k_6)[ClO_2]^2 + k_7}{(3k_5 - k_6)[ClO_2]^2 - k_7} \quad \ldots\ldots\ldots \quad (7)$$

Equation 7 predicts a hyperbolic dependence of τ on $[ClO_2]$ as found experimentally, and a good fit of the expression (not shown) can be made to the data of Figure 1. Curve fitting is not profitable in this case since too many estimates have to be made of the rate constants.

Next we analyze the temperature dependence predicted by equation 7. A limiting case can be examined. In the high temperature and pressure regime of the study, $k_5 \gg k_6$ and $[ClO_2] \gg \sqrt{k_7/(3k_5 - k_6)}$, then $\tau \doteq k_1/3k_2k_a$. For these conditions, the activation energy of Figure 3 will be equal to $(-E_1 + E_2 + E_a)$. Reaction 1 is essentially a radical combination reaction which should have little or no energy requirement. Reaction 2 is a type of radical displacement reaction and the activation energy by Hirschfelder's

rule should be about 5% of the (estimated 4 kcal) bond being broken, or ~0.2 kcal. Thus the measured value of 11.1 kcal should be assigned almost entirely to E_a. This represents the energy barrier to the activated adsorption of reaction a'.

As temperature decreases, τ increases and becomes infinite at ~45°C. The asymptotic approach to this limit is shown in Figure 3. As pressure decreases, equation 7 predicts a lower pressure limit, which the explosion theoretically must have, given by

$$[ClO_2] = \sqrt{k_7/3k_5 - k_6} \quad .$$

This limit must lie below 0.1 - 0.2 Torr, since it was not observed experimentally.

Many other reactions have been considered in the mechanism and all of them have been found to yield results at variance with the experimental observations. We should like to mention just one of these:

$$ClO \xrightarrow[wall]{8} \text{destroyed}$$

This is not excluded as a heterogeneous termination reaction along with but not replacing reaction 7. Including reaction 8, the explosion condition becomes $\phi = \beta/\alpha$ where $\beta = \{ 1 + K_8/k_1[ClO_2] \}$, and the expression for τ (equation 7) is the same but multiplied by the factor

$$\left\{ \frac{k_1[ClO_2] + K_8}{k_1[ClO_2]} \right\}^2$$

This quantity approaches unity at high $[ClO_2]$, but never disappears at any low $[ClO_2]$. Hence reaction 7 is required to make τ infinite when $[ClO_2]$ is extremely low.

E. REFERENCES

1. E. T. McHale and G. von Elbe, J. Am. Chem. Soc., 89, 2795 (1967).

2. G. Porter and F. J. Wright, Disc. Faraday Soc. 14, 23 (1953).

3. S. W. Benson and J. H. Buss, J. Chem. Phys. 27, 1383 (1957).

4. S. W. Benson and K. H. Anderson, J. Chem. Phys. 31, 1082 (1959).

5. Z. G. Szabo, J. Chem. Soc. (London), 1356 (1950).

6. JANAF Thermochemical Tables, The Dow Chemical Co., Midland, Mich., 1964.

7. H.-J. Schumacher and G. Stieger, Z. Physik Chem. B7, 363 (1930).

8. F. E. King and J. R. Partington, J. Chem. Soc. (London), 925 (1926).

9. A. H. Nielsen and P. J. H. Woltz, J. Chem. Phys. 20, 1878 (1952).

10. C. F. Goodeve and J. Powney, J. Chem. Soc. (London), 2078 (1932).

11. C. F. Goodeve and F. D. Richardson, J. Chem. Soc. (London), 294 (1937).

12. F. Kaufman and N. J. Gerri, Eighth Symposium (International) on Combustion, Williams and Wilkins Co., Baltimore, Md., 1962, p. 619.

13. J. Farquharson, C. F. Goodeve, and F. D. Richardson, Trans. Faraday Soc. 32, 790 (1936).

14. H. Booth and J. B. Bowen, J. Chem. Soc. (London) 127, 510 (1925).

15. N. N. Semenov, "Some Problems in Chemical Kinetics and Reactivity," Princeton University Press, Princeton, N. J., 1959, Volume 2.

16. C. F. Goodeve and A. E. Marsh, J. Chem. Soc. (London), 1332 (1939).

17. Z. G. Szabo, Trans. Faraday Soc. 55, 1127 (1959).

18. H.-J. Schumacher, "Chemische Gasreactionen," Theodor Steinkopff, Dresden and Leipzig, Germany, 1938.

19. K. J. Laidler, "Chemical Kinetics," 2nd Edition, McGraw-Hill Book Co., Inc., New York, N. Y., 1964.

20. B. Lewis and G. von Elbe, "Combustion, Flames and Explosions of Gases," 2nd Edition, Academic Press, Inc., New York, N. Y., 1961.

UNCLASSIFIED
Security Classification

DOCUMENT CONTROL DATA - R & D

(Security classification of title, body of abstract and indexing annotation must be entered when the overall report is classified)

1. ORIGINATING ACTIVITY (Corporate author)	2a. REPORT SECURITY CLASSIFICATION
Atlantic Research Corporation Alexandria, Virginia 22314	Unclassified
	2b. GROUP

3. REPORT TITLE

RESEARCH ON THE DEFLAGRATION OF HICH-ENERGY SOLID OXIDIZERS

4. DESCRIPTIVE NOTES (Type of report and inclusive dates)
Final Report - December 15, 1967 (Scientific)

5. AUTHOR(S) (First name, middle initial, last name)
Guenther von Elbe Raymond Friedman
Edward T. McHale Joseph B. Levy

6. REPORT DATE	7a. TOTAL NO. OF PAGES	7b. NO. OF REFS
December 15, 1967	63	26

8a. CONTRACT OR GRANT NO.	9a. ORIGINATOR'S REPORT NUMBER(S)
AF 49(638)-1645	
b. PROJECT NO. 9713-01	
c. 61445014	9b. OTHER REPORT NO(S) (Any other numbers that may be assigned this report)
d. 681308	AFOSR 68-0002

10. DISTRIBUTION STATEMENT
2. This document is subject to special export controls and each transmittal to foreign governments or foreign nationals may be made only with prior approval of AFOSR (SRGO).

11. SUPPLEMENTARY NOTES	12. SPONSORING MILITARY ACTIVITY
TECH, OTHER	Air Force Office of Scientific Research Arlington, Virginia 22209 (SREP)

13. ABSTRACT

This report covers research performed during the past two years on the self-deflagration of hydroxylammonium perchlorate, the general objective of which was to gain some understanding of the combustion process. The experimental work included measurements of the pressure dependence of the deflagration rate, flame temperature, quenching diameters, and inflammability limits. A summary of the significant results of all the solid oxidizers which we have studied is included, and an analysis of the combustion of these monopropellant-type oxidizers is given. The physical and chemical kinetic processes beneath, at and in the gas above the surface of the solid are considered, the concept of cellular flame structure is discussed, and inflammability limits are analyzed.

The scope of the program also included a study of the extinguishment of propellants by rapid depressurization. In this phase of the work we developed a laboratory scale extinguishment apparatus which was essentially a modified optical strand burner. It has the advantages that data are obtained in a form suitable for testing extinction theories and also it can be used to study propellant extinguishment on strand-size sample Three candidate composite propellants were selected for study and the results compared with extinguishment theory.

A study aimed at gaining some background knowledge in the general area of chlorine-oxide chemistry was also undertaken. In this phase of the work an experimental study of the explosive decomposition of chlorine dioxide was performed. The results of the ClO_2 study together with an extensive interpretation of the reaction are presented.

DD FORM 1 NOV 65 1473

UNCLASSIFIED
Security Classification

UNCLASSIFIED

Security Classification

14 KEY WORDS	LINK A		LINK B		LINK C	
	ROLE	WT	ROLE	WT	ROLE	WT
Solid Oxidizers						
Deflagration						
Hydroxylammonium Perchlorate						
Solid Propellant Oxidizers						
Solid Propellant Extinguishment						
Extinguishment						
Extinguishment by Rapid Depressurization						
Chlorine Oxides						
Chlorine Dioxide						
Explosive Decomposition of Chlorine Dioxide						
Degenerate Chain-Branching Explosion						

UNCLASSIFIED

Security Classification